LASER-EXCITED ATOMIC FLUORESCENCE IN A GRAPHITE FURNACE

BY

DOUGLAS EDMON GOFORTH

A DISSERTATION PRESENTED TO THE GRADUATE SCHOOL
OF THE UNIVERSITY OF FLORIDA IN
PARTIAL FULFILLMENT OF THE REQUIREMENTS
FOR THE DEGREE OF DOCTOR OF PHILOSOPHY

UNIVERSITY OF FLORIDA

1986

ACKNOWLEDGMENTS

I would like to express my sincerest gratitude to Dr. James D. Winefordner. His guidance and insight have been extremely beneficial to me. I would like to acknowledge Dr. Benjamin Smith and Dr. Edward Voigtman for their help with my research. I would also like to thank my family for their continual support during my education. Lastly, I would like to thank my friends, who have been an inspiration to me.

TABLE OF CONTENTS

Abstract of Dissertation Presented to the Graduate School
of the University of Florida in Partial Fulfillment of the
Requirements for the Degree of Doctor of Philosophy

LASER-EXCITED ATOMIC FLUORESCENCE
IN A GRAPHITE FURNACE

BY

DOUGLAS EDMON GOFORTH

August, 1986

Chairman: James D. Winefordner
Major Department: Chemistry

Laser-excited atomic fluorescence in a graphite furnace was evaluated while varying different aspects of the graphite furnace and the laser system. The fluorescence system consisted of a nitrogen-pumped dye laser, a graphite cuvette, a monochromator-photomultiplier system, a boxcar averager, and a readout system (chart recorder or computer).

A plain graphite cup, a graphite rod, and a slotted graphite cup were tried as the graphite cuvette. In order to protect the graphite cuvette and also to enhance atomization, a pyrolytic coating, a tantalum carbide layer, a tantalum foil liner, and a calcium matrix which forms a carbide layer were compared as coatings for the graphite cuvette. The plain graphite cup with the pyrolytic coating was found to give the best results for volatile elements. A graphite tube

furnace was evaluated and found to give improved detection limits over the plain graphite cup for nonvolatile elements.

An argon atmosphere, a hydrogen-argon atmosphere, and a low pressure atmosphere were compared as the environment surrounding the graphite furnace. Both the argon atmosphere and the hydrogen-argon atmosphere were found to give very good results.

A copper vapor laser was compared to the nitrogen laser as the pump laser. The high repetition rate (6 kHz) of the copper vapor laser makes it very attractive for use with the transient signal generated by the graphite furnace. However, the copper vapor laser gave mixed results due to inefficent frequency-doubling and also because of losses associated with using a fiber optic for the laser beam.

Overall, most of the detection limits were in the picogram to subpicogram range with an analytically useful range from 3 to 7 orders of magnitude.

CHAPTER 1
INTRODUCTION

Atomic fluorescence spectrometry (AFS) is one of the most sensitive analytical methods for trace analysis. Atomic fluorescence is based on the photon excitation of atoms to an excited state which subsequently undergo radiational deexcitation over a short period of time (order of nanoseconds). The frequencies as well as the intensities of the light emitted by electronically excited atoms are determined by the electronic configurations of the atoms in both their ground and excited states. Therefore, the spectrum of every atom is made up of discrete lines which reflect the electronic structure of that atom.

The fluorescence signal is linearly proportional to the source irradiance until saturation is achieved. Some of the criteria (1) important for choosing an excitation source are high irradiance over the absorption line, good short and long term stability, simplicity of operation, a usefulness for all spectral lines, and a freedom from stray light. Several types of conventional sources have given satisfactory results (2,3): metal vapor discharge lamps, hollow cathode lamps, electrodeless discharge lamps, and xenon arc lamps. Both metal vapor discharge lamps and hollow cathode lamps are relatively low in intensity compared to other sources and therefore have not been used recently.

Prior to lasers, electrodeless discharge lamps were the most used AFS sources (4,5). These sources are tedious to produce and no reliable production and operation methods are available for all elements. The use of these sources has dropped off considerably since the advent of lasers. The xenon arc continuum lamp was used in the early stages of AFS and more recently the Eimac xenon arc lamp was used in several multi-element AFS systems (6,7).

The pulsed, tunable dye laser (8-10) has evolved as the problem solving tool for atomic fluorescence analysis. The dye laser has the following unique features: 1) tunable over the visible wavelength region and with frequency-doubling, covers the region down to 220 nm; 2) extremely high peak powers; 3) coherence, both spatial as well as temporal, thereby leading to high power densities (small spot size) and narrow linewidths (monochromaticity); and 4) pulsed with a low duty cycle so that the maximum benefit of signal-to-noise ratio should be obtained for background noise-limited systems by gated operation.

In almost all cases, the detection system has consisted of a photomultiplier tube and single channel detection. With pulsed laser systems, the most widely used data processing system has been a photomultiplier tube wired for a fast response and a boxcar averager (11). The boxcar averager has a variable gate that can be operated by a reference signal so that information is collected only during the laser firing. In this manner, the background noise is only measured during the short "on" time of the detector.

Laser-excited fluorescence has been applied primarily to atmospheric pressure flames (12-14), electrothermal atomizers (15-25),

and inductively coupled plasmas (ICP) (22,26,27). The results for flames and plasmas have not shown a significant improvement over other analytical techniques (11,28). Flames are limited by scatter caused by unvaporized particles in the atomizer when there is a large excess of matrix (Mie Scattering) (28). Also, native flame species (OH, CH, CN, C_2) or molecular species formed in the combustion process can give rise to a fluorescence background (29). The ICP does not have the scattering or background fluorescence of the flame and has been used in combination with pulsed laser excitation (22) to achieve very low detection limits for refractory elements. However, electrothermal atomizers provide the ultimate sensitivity in analytical laser fluorescence work. For a graphite cuvette, there are increased atomic concentrations because the atomic vapor is maintained in a smaller volume than a flame or ICP, and the graphite cell is essentially a static cell as opposed to a dynamic system like a flame. The graphite furnace also has decreased quenching of radiationally excited atoms. Under ideal conditions, the limiting noise for atomic fluorescence in a furnace should be shot noise from the detector, which is much smaller than the Mie scatter and the flame background flicker noise. One added attraction for the electrothermal atomizer is that solid sampling can be achieved (30).

Theoretical Considerations

Types of Fluorescence Transitions

Various types of atomic fluorescence transitions have been used for analytical studies. Figure 1-1 shows the types of fluorescence transitions. There are basically five types of atomic fluorescence transitions (31). Resonance fluorescence occurs when the same lower and upper levels are involved in the excitation and deexcitation processes. Direct line fluorescence occurs when the same upper level is involved in the excitation and deexcitation processes; however, different lower levels are used. In stepwise line fluorescence, different upper levels are involved in the radiational excitation and deexcitation processes. Sensitized fluorescence occurs when one species is excited (called the donor) and transfers excitation energy to an atom of the same or another species (called the acceptor), either of which deexcites radiationally. Lastly, multiphoton fluorescence results when two or more photons excite an atomic species which then radiationally deexcites.

The fluorescence is termed Stokes if the excitation energy is greater than the fluorescence energy; if the fluorescence energy is greater than the excitation energy, the process is called anti-Stokes. The fluorescence is said to be "excited," if the radiational excitation and fluorescence processes involve only excited states. Thermally assisted fluorescence occurs if the excitation process involves a collisional excitation following the radiational excitation.

Figure 1-1. Types of Atomic Fluorescence: a) resonance; b) excited state resonance; c) Stokes direct-line; d) excited state Stokes direct-line; e) anti-Stokes direct-line; f) excited state anti-Stokes direct-line; g) Stokes stepwise line; h) excited state Stokes stepwise line; i) anti-Stokes stepwise line; j) excited state anti-Stokes stepwise line; k) thermally assisted Stokes or anti-Stokes stepwise line (depending upon whether the absorbed radiation has shorter or longer wavelengths, respectively, than the fluorescence radiation); l) excited state thermally assisted Stokes or anti-Stokes stepwise line (depending upon whether the absorbed radiation has shorter or longer wavelengths, respectively, than the fluorescence radiation); m) sensitized (D = donor, D* = excited donor, A = acceptor, A* = excited acceptor, $h\nu_E$ = exciting radiation, $h\nu_F$ = fluorescence radiation); n) two-photon excitation via a virtual level; o) two-photon excitation via a real level.

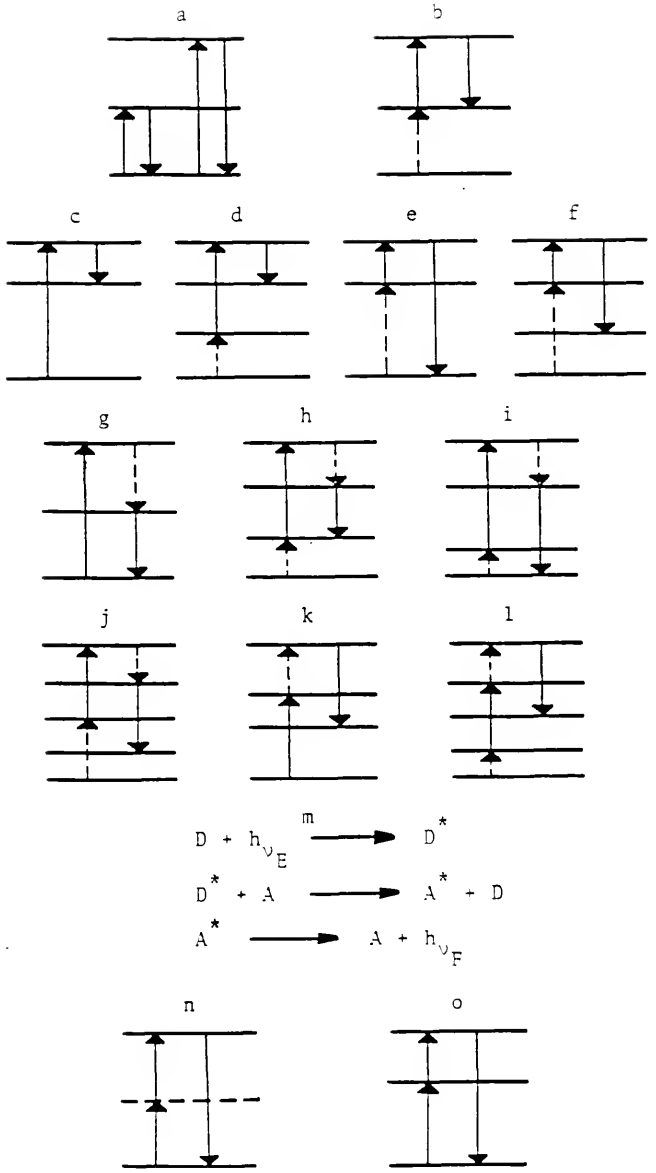
a
b
c
d
e
f
g
h
i
j
k
l
m
$D + h\nu_E \longrightarrow D^*$
$D^* + A \longrightarrow A^* + D$
$A^* \longrightarrow A + h\nu_F$
n
o

Fluorescence Expressions

The treatment of the intensity expressions (1) assumes that there is only a two level system, i.e., ground state, 1, and first excited state, 2. The basic fluorescence radiance expression is given by

$$B_F = (\frac{1}{4\pi})Y_{21}E_{\nu 12}\int_0^\infty k_\nu d\nu \qquad (1)$$

where

l = path length in direction of detection system, m

4π = number of steradians in a sphere, sr

Y_{21} = fluorescence power (quantum) efficiency, W fluoresced/W absorbed

$E_{\nu 12}$ = spectral irradiance of exciting radiation at absorption line, $Wm^{-2}Hz^{-1}$

$k_\nu d\nu$ = integrated absorption coefficient over absorption line, $m^{-1}Hz$.

$$\int_0^\infty k_\nu d\nu = n_1(\frac{h\nu_{12}}{c})B_{12}[1 - \frac{g_1 n_2}{g_2 n_1}],\ m^{-1}Hz \qquad (2)$$

where

n_1 = concentration of analyte atoms, m^{-3}

$h\nu_{12}$ = energy of the exciting photon, J

c = speed of light, ms^{-1}

B_{12} = Einstein coefficient of induced absorption, $m^3J^{-1}s^{-1}Hz$

g_1, g_2 = statistical weights of states 1 and 2, respectively, dimensionless

n_1, n_2 = concentration of states 1 and 2, respectively, m^{-3}, ($n_1+n_2 = n_T$, the total concentration of atoms in all states)

The factor in brackets accounts for the absorption decrease caused by stimulated emission.

Assuming a steady state approach, where the excitation rate equals the deexcitation rate

$$(k_{12} + \frac{B_{12}E_{\nu 12}}{c})n_1 = (k_{21} + A_{21} + \frac{B_{21}E_{\nu 12}}{c})n_2 \tag{3}$$

where

k_{12}, k_{21} = excitation and deexcitation nonradiational (collision) rate constants, s^{-1}

A_{21} = Einstein coefficient of spontaneous emission, s^{-1}

B_{21} = Einstein coefficient of induced emission, $m^3Js^{-1}Hz$

B_{12} = Einstein coefficient of induced absorption, $m^3Js^{-1}Hz$

n_1, n_2 = concentrations of electronic states 1 and 2, m^{-3}

c = speed of light, ms^{-1}

The fluorescence quantum efficiency, Y_{21}, is defined as

$$Y_{21} = \frac{A_{21}}{A_{21} + k_{21}} \tag{4}$$

and A_{21} is related to B_{21} and B_{12} by

$$A_{21} = (\frac{8\pi h\nu^3_{12}}{c^3})B_{21} = (\frac{8\pi h\nu^3_{12}}{c^3})(\frac{g_1}{g_2})B_{12} \tag{5}$$

where h is the Planck constant. Combining these expressions, B_F yields

$$B_F = (\frac{1}{4\pi})Y_{21}E_{\nu 12}[n_1(\frac{h\nu_{12}}{c})B_{12}(\frac{E^*_{\nu 12}}{E^*_{\nu 12} + E_{\nu 12}})] \tag{6}$$

where

$$E^*_{\nu 12} = \frac{cA_{21}}{B_{21}Y_{21}} \tag{7}$$

The saturation spectral irradiance, $E^s_{\nu 12}$ is the source irradiance which results in a fluorescence radiance 50% of the maximum possible value

$$E^s_{\nu 12} = E^*_{\nu 12}(\frac{g_1}{g_1 + g_2}) \tag{8}$$

Making substitutions and also substituting for n_1 in terms of n_T, B_F is given by

$$B_F = (\frac{1}{4\pi})Y_{21}E_{\nu 12}n_T(\frac{h\nu_{12}}{c})[\frac{B_{12}}{1 + \frac{E_{\nu 12}}{E^s_{\nu 12}}}] \tag{9}$$

From these results, several conclusions can be made:

(i) B_F is linear with n_T as long as the optical density is low.

(ii) B_F is linearly dependent upon the source irradiance and the fluorescence quantum efficiency as long as $E_{12} << E^s_{12}$

$$B_F = (\frac{1}{4\pi})Y_{21}E_{\nu 12}n_T(\frac{h\nu_{12}}{c})B_{12} \qquad (10)$$

which is the case for excitation by conventional sources.

(iii) B_F is independent of the source irradiance and the fluorescence quantum efficiency if $E_{\nu 12} > E^s_{\nu 12}$. There is saturation of the upper state and B_F is the maximum possible value for a given n_T

$$B_F = (\frac{1}{4\pi})Y_{21}E^s_{\nu 12}n_T(\frac{h\nu_{12}}{c})B_{12} \qquad (11)$$

or by substituting for $E^s_{\nu 12}$

$$B_F = (\frac{1}{4\pi})h\nu_{12}A_{21}n_T(\frac{g_1}{g_1 + g_2}) \qquad (12)$$

Therefore, the fluorescence is determined by the well known parameters A_{21}, g_1, g_2, $h\nu_{12}$, and by n_T. At high concentrations, the exact expression for B_F becomes very complex. There is also a leveling of the signal due to self-absorption.

Formation of the Atomic Vapor

The purpose of the graphite furnace is to atomize the analyte salt. Various works (32-38) have attempted to determine the atomization mechanism for many different elements. These works were carried out using atomic absorption spectrometry. The measurements

are made more difficult because the possibility of high thermal gradients, the rapid rates of rise of temperatures, and the transient signals by these atomizers (39,40) may not allow local thermal equilibrium.

Sturgeon et al. (37) and Sturgeon and Chakrabarti (38) proposed that there are four potential routes to the atomic species for an analyte in the graphite furnace

$$MO_{s/l} + C \rightarrow M_s + CO_g \rightarrow M_g \tag{13}$$

$$\rightarrow M_{2g} \rightarrow 2M_g \tag{13a}$$

$$MO_s \rightarrow M_g + O_g \tag{14}$$

$$MO_s \rightarrow MO_g \rightarrow M_g + O_g \tag{15}$$

$$MX_s \rightarrow MX_g \rightarrow M_g + X_g \tag{16}$$

where M = metal, O = oxygen, C = carbon, and X = halide. If the sample is in the form of a nitrate or sulfate, the metal oxide usually results on heating. Therefore, the majority of precursors to gas phase atoms are metal oxides or metal halides. The appearance temperature (temperature of the furnace at which the signal begins) was used as an indication of E_a, the bond dissociation energies of gaseous species. By determining the precursors to the analyte atoms, they could predict the atomization mechanism. Other works (41-43) have suggested that the thermal dissociation of the carbide is an important mechanism for the refractory elements

$$MC_{s/l} \rightarrow M_g + C_s \qquad (17)$$

High dissociation energies of carbides are responsible for the high atomization temperatures required for such elements as Mo and V.

The analyte concentration (3,44) within furnace atomizers depends upon the sample characteristics, the rate of heating of the furnace, the thickness of the sample on the furnace walls, and the environment within and type of furnace. Although there are mathematical models (38,45,46) describing the time-dependent characteristics of the atom population within a furnace, they do not attempt to take into account any experimental parameters. Holcombe and Rayson (47) used a Monte Carlo simulation to model the release of Ag atoms from the surface of the graphite. The data supported the proposed mechanisms (48) for the vaporization of Ag in a graphite furnace.

Losses of the atomic vapor (47,49) include diffusion out of the ends of the (tube) furnace, diffusion out of the sample injection port, and losses through the graphite walls. A pyrolytic coating on the graphite (50-52) is utilized most often to minimize losses of analyte through the graphite walls. Some chemical interferences include the formation of volatile halides (53,54) and oxides (55) with the analyte atoms. Matrix modifiers have been used to minimize the losses of halides and addition of hydrogen to the sheath gas has reduced interferences from oxides.

Review of Literature

The first analytical use of atomic fluorescence was in the 1960s by Winefordner and Vickers (56) using a flame as the atomizer and a metal vapor discharge lamp as the source. Since that time, atomic fluorescence has utilized the sources and atomizers previously discussed. General reviews on atomic fluorescence are given by Winefordner et al. (3), Browner (57), Sychra et al. (2), Wineforder (1,58,59) and Omenetto and Winefordner (60). Omenetto and Winefordner (61) have given a review of applications for laser fluorescence, and Omenetto and Human (11) have given some general considerations for laser fluorescence.

Most of the graphite cells for atomic absorption have been based on the L'vov furnace (62). Massmann (63) first demonstrated the usefulness of graphite cells for atomic fluorescence spectrometry. His cell consisted of a cup shaped graphite cuvette in which the source radiation enters through the top and the fluorescence is viewed through a slit cut into its wall. West and Williams (64) constructed a carbon filament (1-2 mm diameter) within a chamber with quartz windows. These early works as well as other furnace designs (65,66) used conventional light sources. A review of fluorescence electrothermal atomizers is given by Winefordner (67), and general reviews on electrothermal atomizers are given by Kirkbright (68) and Wineforder and Vickers (69).

More recently, many workers (15-25) have utilized lasers as the excitation sources for furnace atomic fluorescence. The pulsed dye laser is the most versatile laser source for atomic fluorescence. In

the work of Bolshov et al. (19), the fluorescence of atoms above a graphite cup furnace was excited by a Nd:YAG-pumped dye laser. The fluorescence was sent to a broadband amplifier and fed into a gated voltmeter (boxcar averager). The best ever detection limits were obtained for Pb, Fe, Na, Pt, Ir, Eu, Cu, Ag, Co, and Mn (most notably 2 fg of Pb).

Using a similar system but with a nitrogen-pumped dye laser, Tilch et al. (23) achieved a detection limit of 5 fg of lead. Human et al. (22) also achieved a 5 fg detection limit for Pb with an excimer-pumped dye laser. Using a graphite boat, Hohimer and Hargis (17) found a detection limit of 2 pg for cesium.

Slightly varied systems include using tungsten spiral atomizers (24) or graphite tubes (25). Miziolek and Willis (20) studied lead using double-resonance fluorescence spectroscopy. Greenlees et al. (70) recorded bursts of six or more fluorescence photons in about 1 s when a single Na or Ba atom passed through their continuous wave laser beam in a vacuum. In a similar experiment, Pan et al. (71) measured sodium atoms and their motion through the laser beam in 200 torr of helium gas.

CHAPTER 2
AN OPEN FURNACE SYSTEM SURROUNDED BY ARGON AND HYDROGEN

Much of the work utilizing laser-excited atomic fluorescence in a furnace has been carried out in an argon atmosphere. Amos et al. (65) have also found that having a hydrogen flame surrounding the graphite burns up any entrained oxygen, thus giving a much more reducing atmosphere for the atomization process. This section describes a furnace system that was open to the atmosphere, but with an argon sheath and a hydrogen flame gas. The main focus of this section was to determine the best graphite cuvette design and also to see if varying the atomizer surface could improve detection limits.

The experimental system described below generally applies to this entire work. Modifications that took place will be described as they occurred.

Experimental

The general experimental system used for all experiments is shown in Figure 2-1 and the components are described in Table 2-1. The basic setup can be divided into three parts: the laser system, the furnace system, and the detection system.

Laser System

The nitrogen-pumped dye laser (Model DL-II dye laser, Molectron; UV-24 nitrogen laser, Molectron, Palo Alto, CA) was operated at 20 Hz

Figure 2-1. Experimental System for Laser-Excited Atomic Fluorescence in a Graphite Furnace.

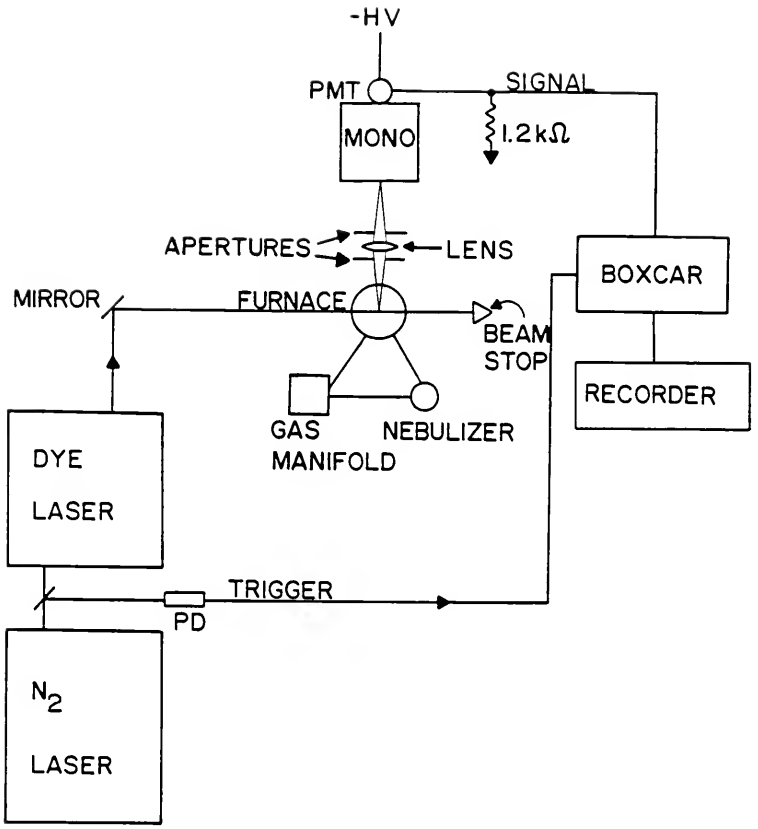
-HV
PMT
SIGNAL
MONO
1.2kΩ
APERTURES
LENS
BOXCAR
MIRROR
FURNACE
BEAM
STOP
RECORDER
GAS
MANIFOLD
NEBULIZER
DYE
LASER
TRIGGER
PD
N2
LASER

Table 2-1
List of Equipment for Fluorescence System

Equipment	Manufacturer
Model DL-II Dye Laser	Molectron Corp., 928 East Meadow Dr., Palo Alto, CA 94303
UV-24 Nitrogen Laser	Molectron Corp., 928 East Meadow Dr., Palo Alto, CA 94303
Furnace and Controlling Circuit	Laboratory Built
Model SCR 20-250 Power Supply for Furnace	Electronics Measurements, 405 Essex Rd., Neptune, NJ 07753
Model EU-700 Scanning Monochromator	Heath,[a] 530 Main St., Acton, MA 01720
Nebulizer	Perkin-Elmer Corp., Main Ave. (MS-12), Norwalk, CT 08846-258
R1414 Photomultiplier Tube	Hamamatsu, 420 South Ave., CN420, Middlesex, NJ 06856
Model 280 High Voltage Power Supply	Princeton Applied Research, P.O. Box 2565, Princeton, NJ 08540
Model 162 Boxcar Averager with a 164 plug-in	Princeton Applied Research, P.O. Box 2565, Princeton, NJ 08540
Model 562-126 Frequency Doubling Crystals	INRAD, 181 Legrand Ave., Northvale, NJ 07647
Model D-5000 Chart Recorder	Houston Instruments, 8500 Cameron Rd., Austin TX 78753
Photodiode Trigger	Laboratory Built

[a]Now GCA/McPherson.

for the experiments with the hydrogen-argon (H_2-Ar) atmosphere. The laser had a spectral line width of 0.015 nm (full width half maximum, FWHM), a pulse width of 5 ns, and a typical pulse energy of 0.3-0.8 mJ in the fundamental region (360-1100 nm). The dye laser was equipped with a frequency-doubling system which allowed frequency-doubling in the range of 220-360 nm and a pulse energy of 5-40 μJ. Since replacement crystals were difficult to obtain from Molectron, during the course of this research this system was replaced by an external frequency-doubling system (Model 562-126, INRAD, Northvale, NJ) which gave similar output characteristics.

The laser beam was allowed to diverge over a 2 m distance to the atomizer. The fundamental beam had a diameter of about 2 mm at the atomizer; the frequency-doubled beam had a diameter of 6 mm at the atomizer due to optics associated with the frequency-doubling system. The radio frequency interference from the nitrogen laser was reduced to a negligible level by enclosing the laser in a well grounded brass screen Faraday cage.

A laboratory built flowing dye system was used for dye circulation. The flowing dye system provided several advantages over the static cell system. Higher repetition rates (e.g., 30 Hz) could be used because of the large volume of dye and also because the dye moved very rapidly through the dye cuvette. In the static system, only 2 mL of dye were confined in the dye cuvette; here, the higher repetition rates caused thermal distortion of the dye and a reduction in beam quality. Also, because of the larger volume (50 mL) of dye in

the flowing dye system, the dye would last much longer before it required changing.

When changing dyes, the flowing dye system was flushed at least five times with solvent. If the solvent for the new dye was different, the new solvent was flushed through the system several times. Finally, the new dye was rinsed through the system once before filling the system with new dye.

Table 2-2 lists the dyes (Exciton, Dayton, OH) used during the course of this research. The dyes all had sufficient lifetimes (~2 hours of operating time) that there was no significant degradation in energy per pulse while running a calibration curve. The dye laser was turned on only during the atomization cycle of the furnace, thus extending the lifetime of the dye even more.

Furnace System

The furnace system (Figure 2-2) was similar to that of Wittman (21) and consisted of a cylindrical phenolic block with water cooled copper blocks on either side to support the graphite electrodes and provide electrical contact with the SCR power supply (SCR 20-250, 5kW, Electronics Measurements, Neptune, NJ). The gas flow control system consisted of one solenoid valve for the sheath and flame diluant gases (argon) and one solenoid valve for the flame gas (H_2). Since the flame gas was only used during the atomization stage, the solenoid switch was very convenient for controlling the gas. The flame gas and the flame diluant gas were fed through a capillary burner below the center of the graphite cuvette. Concentric rings surrounding the capillary burner allowed the sheath gas to cover the entire length of

Table 2-2
Dyes Used in N_2-Pumped Dye Laser

Dye	Concentration (M)	Solvent	WL Range (nm)	Freq. Dbl. WL Range (nm)
PBBO	$2.3X10^{-3}$	p-dioxane	388-417	
BBQ	$1.0X10^{-3}$	p-dioxane	365-407	
Coumarin 540A	$1.0X10^{-2}$	ethanol	515-583	258-291
Rhodamine 590	$5.0X10^{-3}$	ethanol	570-630	285-315
Rhodamine 610	$3.7X10^{-3}$	ethanol	593-646	297-323
Rhodamine 640	$5.7X10^{-3}$	ethanol	620-673	310-336
Oxazine 720	$1.0X10^{-3}$	ethanol	658-723	329-362

Figure 2-2. Configuration of Furnace for the Hydrogen-Argon Atmosphere.

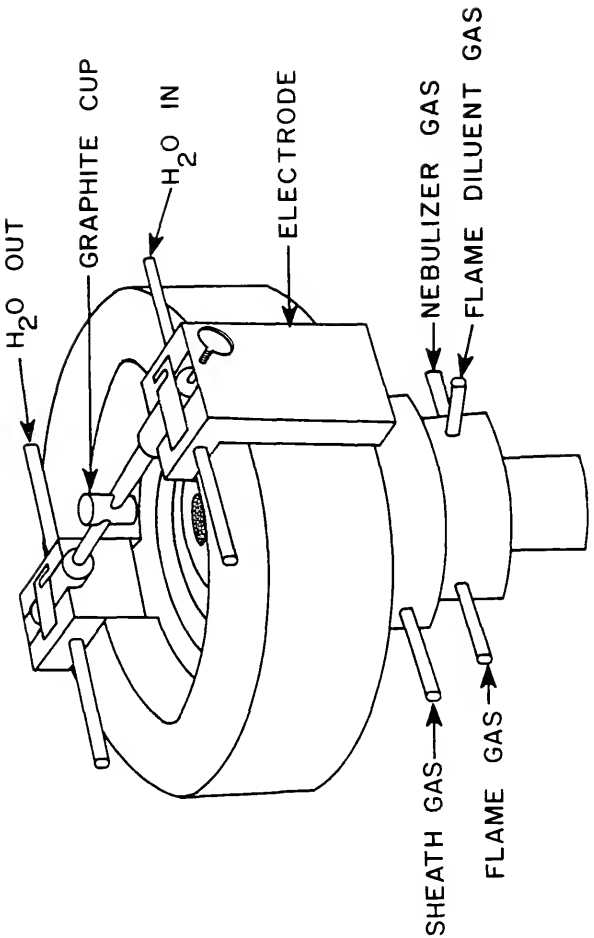
H_2O OUT
GRAPHITE CUP
H_2O IN
ELECTRODE
NEBULIZER GAS
FLAME DILUENT GAS
SHEATH GAS
FLAME GAS

the graphite cuvette, thus protecting the cuvette from the atmosphere. As the graphite cuvette heated up during the atomization cycle, the hydrogen would ignite, burning up any entrained oxygen. The gas flow rates were ca. 3 L/min of argon sheath gas, 2 L/min of argon flame diluant, and 1 L/min of the hydrogen flame gas. Each gas had its own rotameter that was calibrated with a mass flow meter (ALK-50K, Hastings, Hampton, VA). A plain graphite cup was used as the cuvette for all of the reported results.

The heating rate and the final temperature of the graphite were controlled by the voltage setting on the power supply and also by a timing circuit. Figure 2-3 shows a simplified diagram of the timing circuit used. The power supply was programmed so that the output was linear with the resistance in the controlling circuit (72), with 100 Ω corresponding to full power. The length of heating time was controlled by a timer chip (555, Texas Instruments, Dallas, TX) which controlled a relay (W171DIP-12, Magnecraft, Chicago, IL). The normally closed (NC) relay pins were in parallel with a 100 Ω resistor. This parallel circuit was in series with a 0-25 Ω variable resistor. The circuit was then connected to two programming inputs on the power supply.

With the switch of the relay in its normally closed position, there was no significant resistance in the controlling circuit. The drying cycle was controlled manually by the 0-25 Ω variable resistor. After drying, a pushbutton was used to initiate the atomization cycle. When the 555 timer was started, it sent a signal activating the relay. The normally closed switch was opened, causing

Figure 2-3. Furnace Power Supply Controlling Circuit. NO = Normally open, NC = Normally closed, 555 Timer = LM 555, Relay = Magnecraft W171 DIP-12, R_T = 0-5 MΩ, C_T = 10 μF.

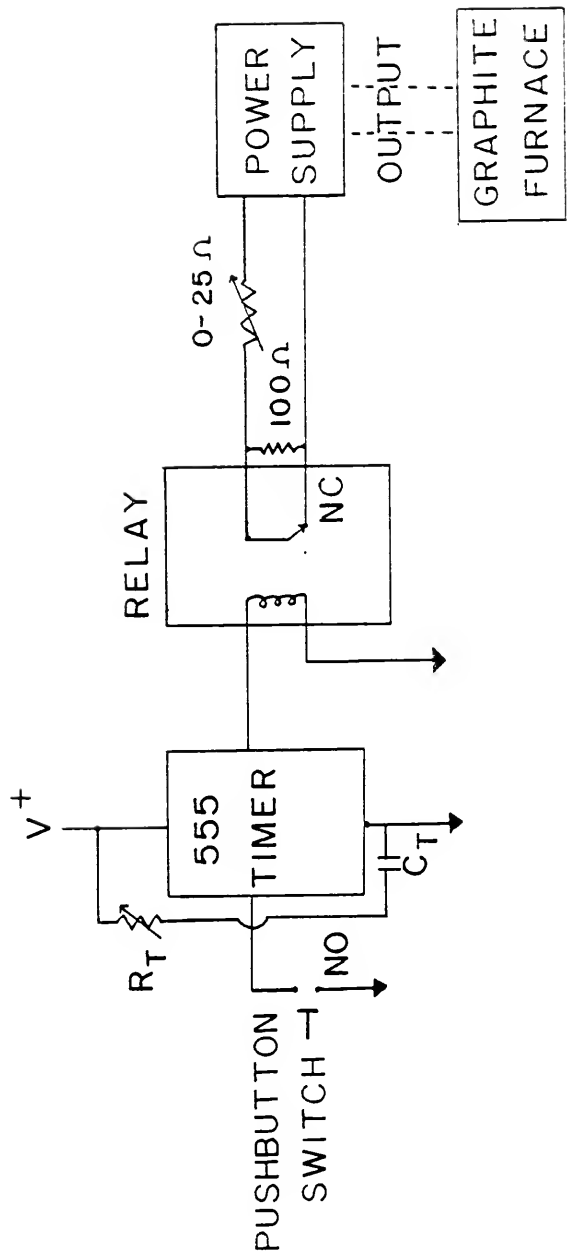
V+
555 TIMER
R_T
C_T
PUSHBUTTON SWITCH
NO
RELAY
NC
100 Ω
0-25 Ω
POWER SUPPLY
OUTPUT
GRAPHITE FURNACE

the 100 Ω resistance in the controlling wires of the power supply, and thus initiating the set maximum output power on the power supply. The amount of time the system was activated was controlled by the timing capacitor, C_T (10 μF), and the timing resistor, R_T (0-5 MΩ). A variable resistor was used for R_T so that the atomization time could be varied between 0 and ~5 s. By setting the maximum output voltage on the power supply and also setting the atomization time with R_T and C_T, the graphite cuvette could be reproducibly heated up to any specified temperature. The temperature of the graphite cuvette was measured with an optical pyrometer (Model 87C, Pyro, Bergenfield, NJ).

Detection System

A lens (1.5 in dia., 2 in F.L.) and aperture system was used to project a 1:1 image of the fluorescence into the monochromator (0.35 m Heath monochromator, stray light--0.1%). The fluorescence was collected at 90° from the laser beam. A tent of black felt placed around the furnace and monochromator helped to reduce stray light. The fluorescence was detected with a photomultiplier tube (Model R1414, Hamamatsu, Middlesex, NJ) mounted within a well-shielded laboratory constructed housing. The photocurrent pulse was stretched slightly by a 1200 Ω load resistor (FWHM 100 ns) and connected directly to a boxcar averager (Model 162 with a 164 plug-in, Princeton Applied Research, Princeton, NJ) operated with a 5 ns gate. The boxcar was triggered by a photodiode which received a fraction of the nitrogen laser output. The boxcar output was displayed on a chart recorder; peak height measurements were made.

Procedure

The stock solutions were prepared in accordance with the directions of Smith and Parsons (73). The standards were prepared from serial dilution of the stock solutions.

Solution samples of 5 µl were deposited using an Eppendorf micropipette. The analyses were carried out with a drying stage for 20 s at 100°C. During the atomization stage, the temperature was set for the specific element up to 2700°C. When necessary, neutral density filters were placed between the furnace and the monochromator to avoid saturating the detection system. The monochromator slit width was varied between 300 µm and 1500 µm.

After optimization of the experimental setup and conditions, analytical calibration curves were obtained for each element. The limit of detection, LOD, was defined as the concentration of analyte producing a signal which was 3X the standard deviation of the blank.

Analysis of Graphite Cuvettes

The atomizer required a special design for atomic fluorescence since the fluorescence was viewed at 90° to the laser beam. A graphite cup (19,23), a Massmann cup (63), a graphite tube with holes cut in the sides (25), and a graphite rod (21,64) are several designs that have been tried. The simplicity of the graphite rod makes it attractive for use with volatile elements. On the other hand, the graphite cup offers an improvement over the graphite rod because the sample is in a semi-enclosed environment which gives more of a "furnace" effect. However, the atoms still have to emerge from the

furnace into the cooler atmosphere before being excited by the laser. As the atoms vaporize out of the hot furnace they have more of a chance to react with interferents, such as O_2. In principle, the best atomizers are those which contain the atoms in a hot environment while they are being excited by the laser. The graphite tube with holes cut in the sides (25) and the Massmann cup (63) are both examples of this type.

Before any data were taken, a preliminary investigation was carried out to determine the best graphite cuvette design. In Figure 2-4, the designs evaluated are shown. For the plain cup and the rod, the laser beam was directed over the top of the cuvette, and the fluorescence was viewed at 90°. For the slotted cup, the laser was directed into the cup from above and the fluorescence viewed through the slots on the side of the graphite cup. The graphite cups were held between two spring-loaded graphite electrodes. These electrodes firmly held the cups and helped to give good electrical contacts.

Analysis of Graphite Coatings

Importance of Graphite Coatings

Electrically heated graphite atomizers have found widespread use in atomic absorption and atomic fluorescence. Unfortunately, in many cases, full advantage cannot be taken of the high temperatures. The tubes rapidly deteriorate and a frequent use of standards is necessary due to a steadily changing response.

Several studies in graphite furnace atomic absorption have utilized coatings to inhibit reactions between the analyte and the

Figure 2-4. Graphite Cuvette Designs.

GRAPHITE CUVETTES

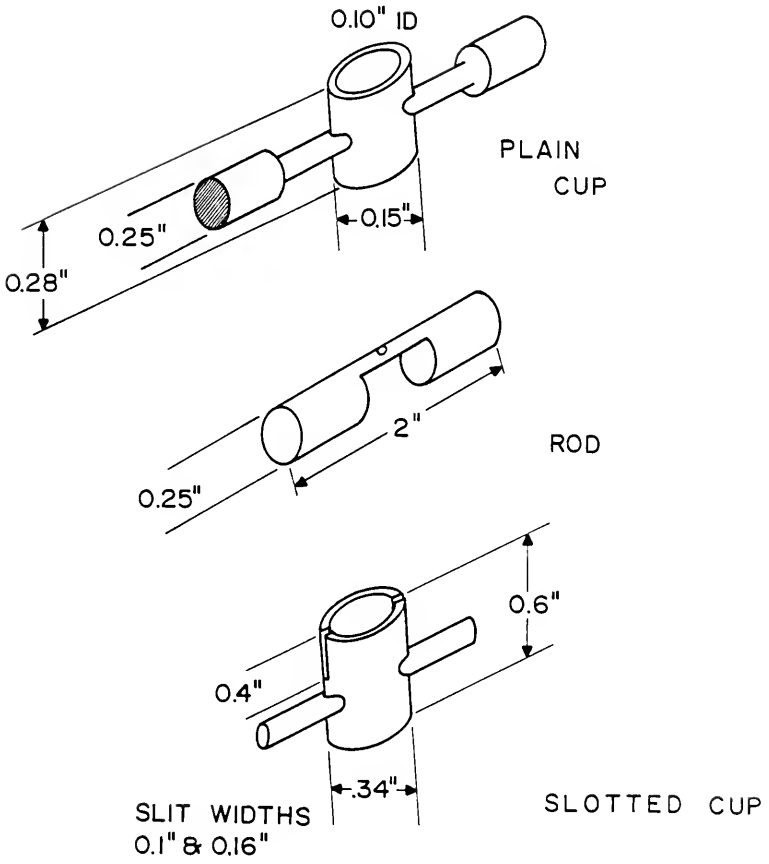

graphite. A pyrolytic coating has been the most popular (50-52). Some alternate coatings include a tantalum treated graphite tube (74), a molybdenum treated graphite tube (75), tantalum foil liners (76-78), metal atomizers (24), and a calcium matrix in the standards (79).

In this study, a pyrolytic coating (Pyro), a tantalum carbide coating (Ta), a calcium matrix which formed a carbide layer (Ca), and a tantalum foil liner (Foil) were compared. A pyrolytic coating has the beneficial properties of low permeability to gases, low porosity, and a resistance to oxidation. The tantalum carbide layer also prevents interaction between the analyte and the graphite. The calcium matrix preferentially forms a calcium carbide layer which protects the graphite much the same as the Ta carbide layer. When using tantalum foil, there is a reduction in diffusional losses of the analyte through the graphite wall. There is a prevention of involatile carbide formation. Finally, analyte compound is reduced by the tantalum to the analyte element.

Coating Procedure

The graphite was pyrolytically coated in a quartz and graphite chamber (Figure 2-5). The "coating" gas used for this process consisted of 90% argon and 10% methane (P-10 gas). The graphite was heated to 2500°C for 10 min while the "coating" gas was flowing through the chamber at about 13 L/min. The "coating" gas continued to flow during a 5 min cooling off period.

The tantalum carbide treatment was the same as that of Zatka (74). The 6% tantalum soaking solution was prepared by weighing 3 g of tantalum metal into a 100 mL PTFE beaker, adding 10 mL of 1/1,

Figure 2-5. Pyrolysis Chamber.

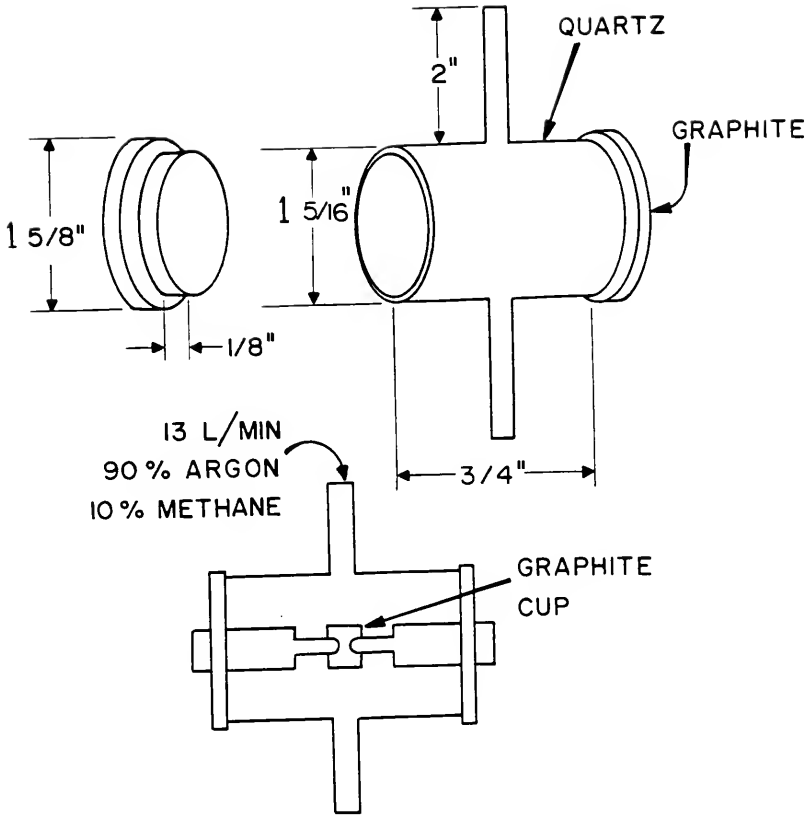
QUARTZ
2"
GRAPHITE
1 5/16"
1 5/8"
1/8"
13 L/MIN
90 % ARGON
10 % METHANE
3/4"
GRAPHITE
CUP

v/v hydrofluoric acid, 3 g of oxalic acid dihydrate, and 0.5 mL of 30% hydrogen peroxide. The solution was carefully heated to dissolve the metal. More peroxide was added if the reaction became too slow. When dissolution was complete, 4 g of oxalic acid and approximately 30 mL of water were added. The acid was dissolved, and the solution diluted to 50 mL. The solution was stored in a plastic bottle.

The graphite cuvettes were then immersed in the 6% tantalum soaking solution in plastic vials. The vials were placed in a desiccator and then evacuated by a water pump for 20-30 s. Atmospheric pressure was then restored in the desiccator, the graphite cuvettes were removed from the soaking solution and dried first in air (30 min) and then at 105°C (1 h). Each cuvette was then placed in the furnace system and heated gradually (30 s) to 1000°C and then for a few seconds to 2500°C. The treatment was repeated again but the tubes were soaked for only 10 s under reduced pressure.

The third method consisted of lining the inner surface of the graphite cup with 0.025 mm thick tantalum foil. The liner was shaped around a smaller metal rod and then allowed to expand in the cup. The cup was then taken through several heating cycles which caused the liner to expand so that there was no clearance between the liner and the cup.

The fourth method consisted of making the standards in a 1000 ppm Ca (as the nitrate) matrix (79). The samples were measured in a pyrolytically coated graphite cup. An ashing step was included to decompose the calcium nitrate to calcium oxide. A temperature of 600°C was used for this step.

Results and Discussion

Choice of Graphite Cuvette

From the preliminary study concerning graphite cuvettes, the plain graphite cup was found to give the best results. The graphite rod worked well with volatile elements, but with the less volatile elements, atomization was inefficient; the sample was vaporized off of the graphite without benefit of a semi-enclosed furnace, which provides higher temperatures inside the furnace. Also, the graphite rod could only hold 2 μL samples and had a tendency to crack at high temperatures.

The slots on the slotted cup were cut in opposite sides of the cup. These slots allowed the fluorescence to be viewed through one slot while the opposite slot reduced the emission from the hot graphite which was directly viewed by the spectrometer. In this way, atoms were still in the hot environment of the cup when they were excited by the laser. Even with the opposite slot for reducing the emission from the luminous graphite, the measured emission still swamped fluorescence signals in the visible region. Extra apertures placed between the atomizer and the monochromator were of little help. Enlarging the width of the slots on the graphite did not help appreciably either. Another problem was the scatter caused by the laser hitting the bottom of the cup. If the excitation and fluorescence lines were close together, the background scatter was very large. Therefore, the plain graphite cup was used; the best results were obtained even though there was a chance for interferences because of cooling of atoms as they exited the graphite cup.

Comparison of Graphite Coatings

Table 2-3 lists the limits of detection (LODs) obtained for the different graphite coatings. Figures 2-6, 2-7, and 2-8 show the log signal versus log concentration calibration curves for Al, Mn, and Cu, respectively. The bending over of the curves at high concentrations was due to self-absorption. The pyrolytic coating gave the best overall results for the elements that were measured. These results were expected since the pyrolytic coating has been shown before (44) to give the best overall results.

The calcium matrix detection limits were all slightly worse than for the pyrolytically coated graphite. The reason for this was that the Ca matrix resulted in a much larger scatter signal even with the ashing step, than the other methods. Any carbide layer that may have formed did not help to enhance the signal.

Except for Al, the Ta foil gave worse detection limits than the pyrolytic coating and also produced calibration curves that were nonlinear. Possible reasons for this were that the foil caused more scatter than the graphite, giving a large background signal. Also, the foil liner seemed to degrade much faster than the other coatings. As the condition of the Ta foil worsened, the efficiency of atomization became poorer. This condition could have accounted for the low slope of the Mn calibration curve and also the relatively short analytically useful range (AUR) for Al, when using the foil liner. Another possible reason for nonlinearity of the calibration curve was that the foil is known to adsorb oxygen very easily (77). The adsorbed oxygen occupied active sites at which atomization can

Table 2-3
Limits of Detection (pg) by Laser-Excited Atomic Fluorescence
for Various Coatings of a Graphite Furnace (5 μL aliquots)

Coating	Al[a]	Mn	Cu
Pyrolytic	$5.X10^{2}$	$7.X10^{0}$	$7.X10^{0}$
Ta Foil	$3.X10^{2}$	$1.X10^{2}$	$6.X10^{1}$
Ta Carbide	$1.X10^{2}$	$1.X10^{1}$	$5.X10^{1}$
Ca Matrix	$7.X10^{2}$	$3.X10^{1}$	$4.X10^{1}$

[a]Limit of detection is defined as 3 σ/m, where σ = standard deviation of the blank and m = slope of calibration curve.

Figure 2-6. Log Intensity vs. Log Mass for Al Utilizing Different Coatings. Slopes: Pyro = 0.98, Ca = 1.03, Ta = 1.06, Foil = 0.95. Typical RSD for each point is 10%.

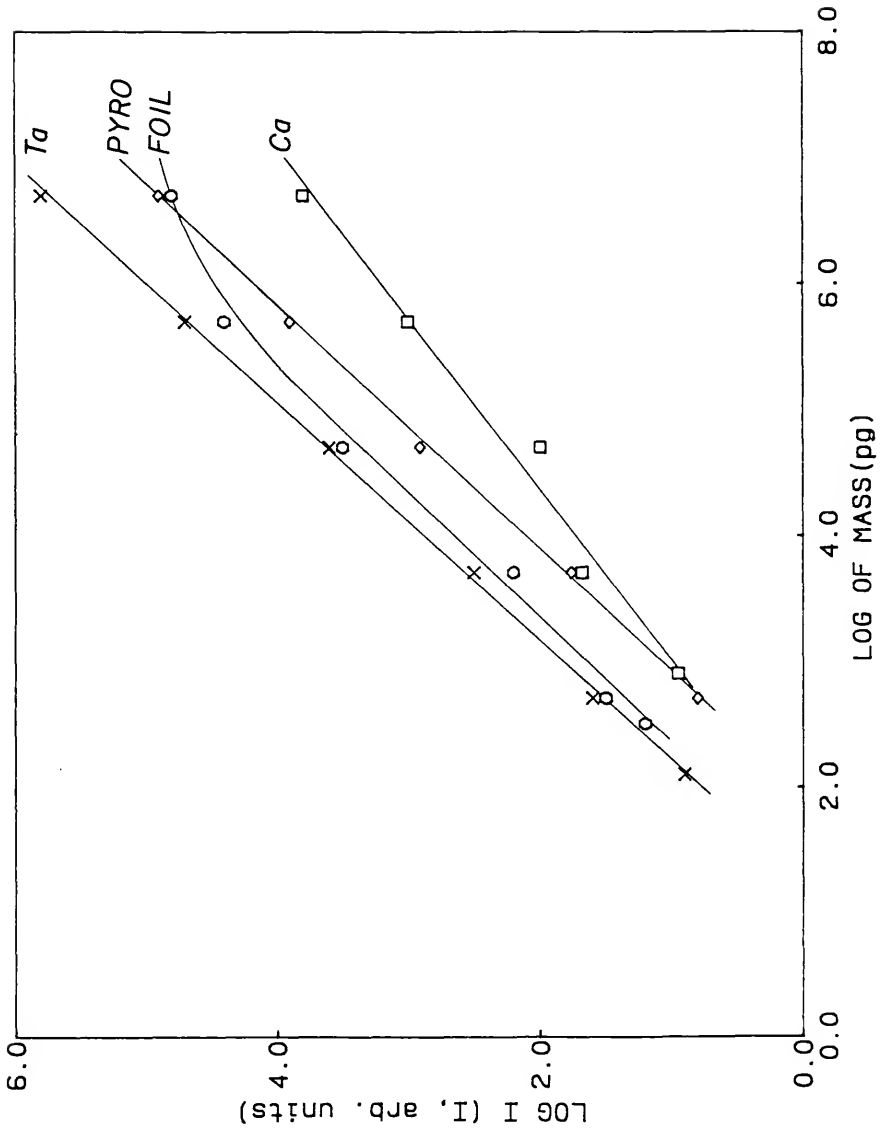
Ta
PYRO
FOIL
Ca
LOG I (I, arb. units)
LOG OF MASS(pg)
0.0
2.0
4.0
6.0
8.0

Figure 2-7. Log Intensity vs. Log Mass for Mn Utilizing Different Coatings. Slopes: Pyro = 0.98, Ca = 0.99, Ta = 1.00, Foil = 0.80. Typical RSD for each point is 10%.

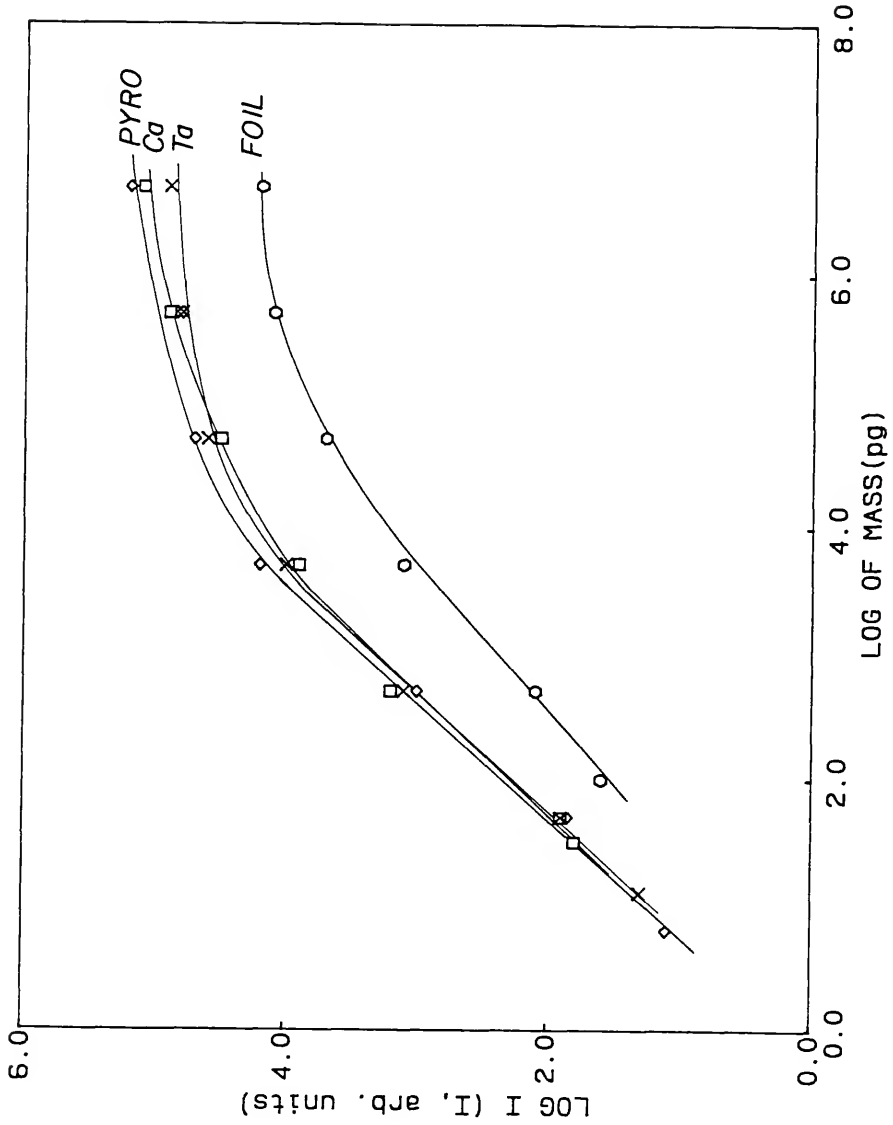
PYRO
Ca
Ta
FOIL
LOG I (I, arb. units)
LOG OF MASS(pg)
0.0
2.0
4.0
6.0
8.0

Figure 2-8. Log Intensity vs. Log Mass for Cu Utilizing Different Coatings. Slopes: Pyro = 0.91, Ca = 0.95, Ta = 0.95, Foil = 1.30. Typical RSD for each point is 10%.

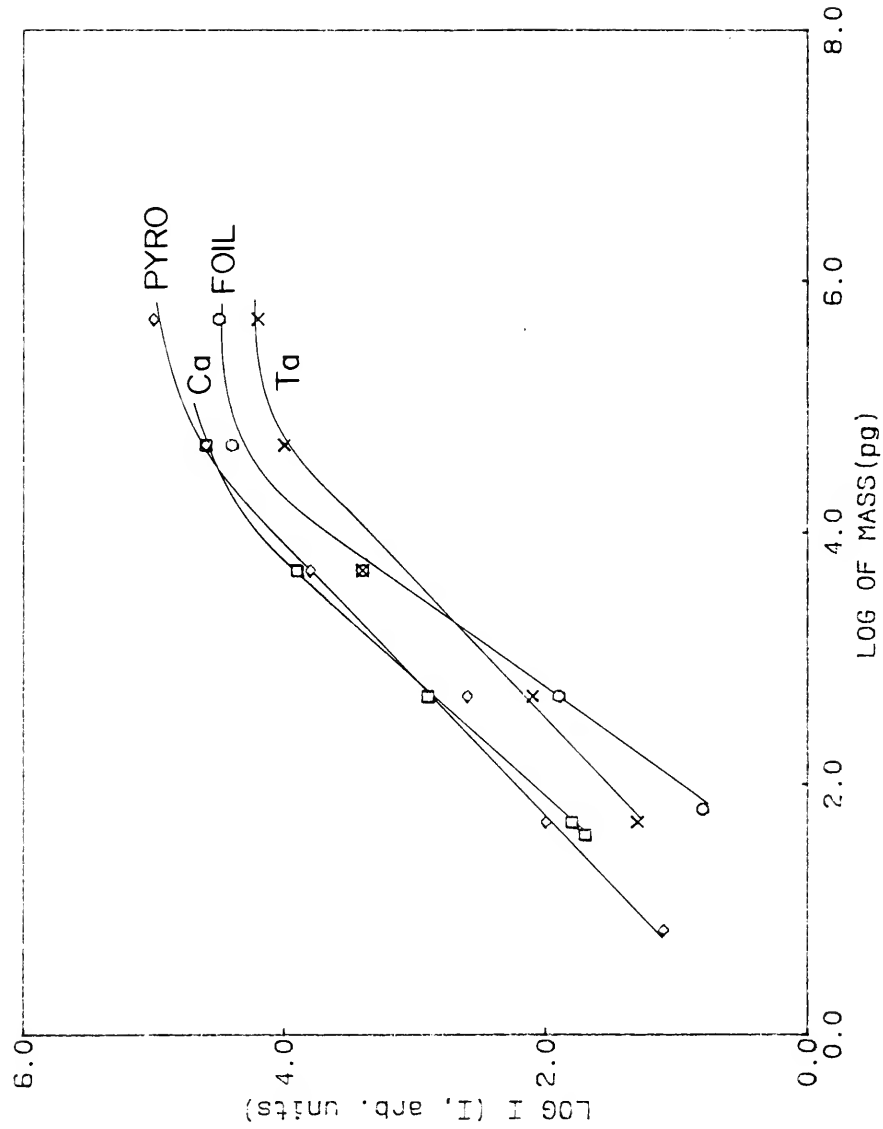
PYRO
FOIL
Ca
Ta
LOG I (I, arb. units)
LOG OF MASS(pg)
0.0
2.0
4.0
6.0
8.0

take place. The oxygen would be removed after several heating cycles, but the lowest concentration may have given uncharacteristically low responses before the oxygen was removed. The atomization mechanism for each of these elements (37,78) would determine whether any of these possible interferents would actually cause any problems.

The Ta carbide coating worked much better than the Ta foil liner. The detection limits were not only improved, but also the AUR and the linearity of the calibration curves were improved. The improved detection limits for Al also suggest that this coating may work well with some of the more refractory elements. For refractory elements, the atomization process has to compete favorably with carbide formation. The Ta carbide layer precludes subsequent carbide formation, thereby enhancing the atomization efficiency.

The pyrolytically coated and the carbide coated cups gave analytically useful results for about 70 atomizations. On the other hand, the Ta foil lined cups would last only about 50 atomizations. All three cups gave a reproducibility of about 10%.

Comparison with Previous Studies

In Table 2-4, LODs obtained in this work are compared with other literature values for the same technique and also furnace atomic absorption spectrometry. Figure 2-9 shows the log-log calibration curves in the H_2-Ar atmosphere. The LODs for Sn, Pt, and In are similar or improved over previous works. The limiting noise in these cases was the photomultiplier dark current. The blank scatter was very small due to the relatively large separation in the excitation

Table 2-4
Limits of Detection (pg) by Laser-Excited Atomic Fluorescence in a Graphite Furnace (5 μL aliquots)

Element	Wavelength (nm)		LAFS[a]		GFAAS[c]
	Exc.	Fl.	This Study	Lit.[b]	
In	410.2	451.1	$5.X10^{-2}$	$1.X10^{-1}$	NR[d]
Sn	286.3	317.5	$2.X10^{-1}$	$5.X10^{2}$	$2.X10^{1}$
Pb	283.3	405.8	$2.X10^{-1}$	$2.X10^{-3}$	$5.X10^{0}$
Mn	279.8	280.1	$7.X10^{0}$	$2.X10^{-1}$	$4.X10^{-1}$
Cu	324.8	327.4	$7.X10^{0}$	$2.X10^{-1}$	$2.X10^{0}$
Pt	265.9	270.2	$6.X10^{1}$	$1.X10^{2}$	$2.X10^{1}$
Al	394.4	396.2	$5.X10^{2}$	NR[d]	$1.X10^{0}$

[a]Laser-excited atomic fluorescence with a graphite furnace. Limit of detection is defined as 3 σ/m, where σ = standard deviation of the blank and m = slope of calibration curve.

[b]Data for In and Sn from (23); Pb, Mn, Cu, and Pt from (19).

[c]Data from (80).

[d]NR = No Report.

Figure 2-9. Log Intensity vs. Log Mass When Using the Hydrogen-Argon Atmosphere. Slopes: Al = 1.04, Mn = 0.98, Cu = 0.91, Pt = 0.93, Sn = 1.00, In = 1.10, Li = 0.90, Pb = 0.80. Typical RSD for each point is 10%.

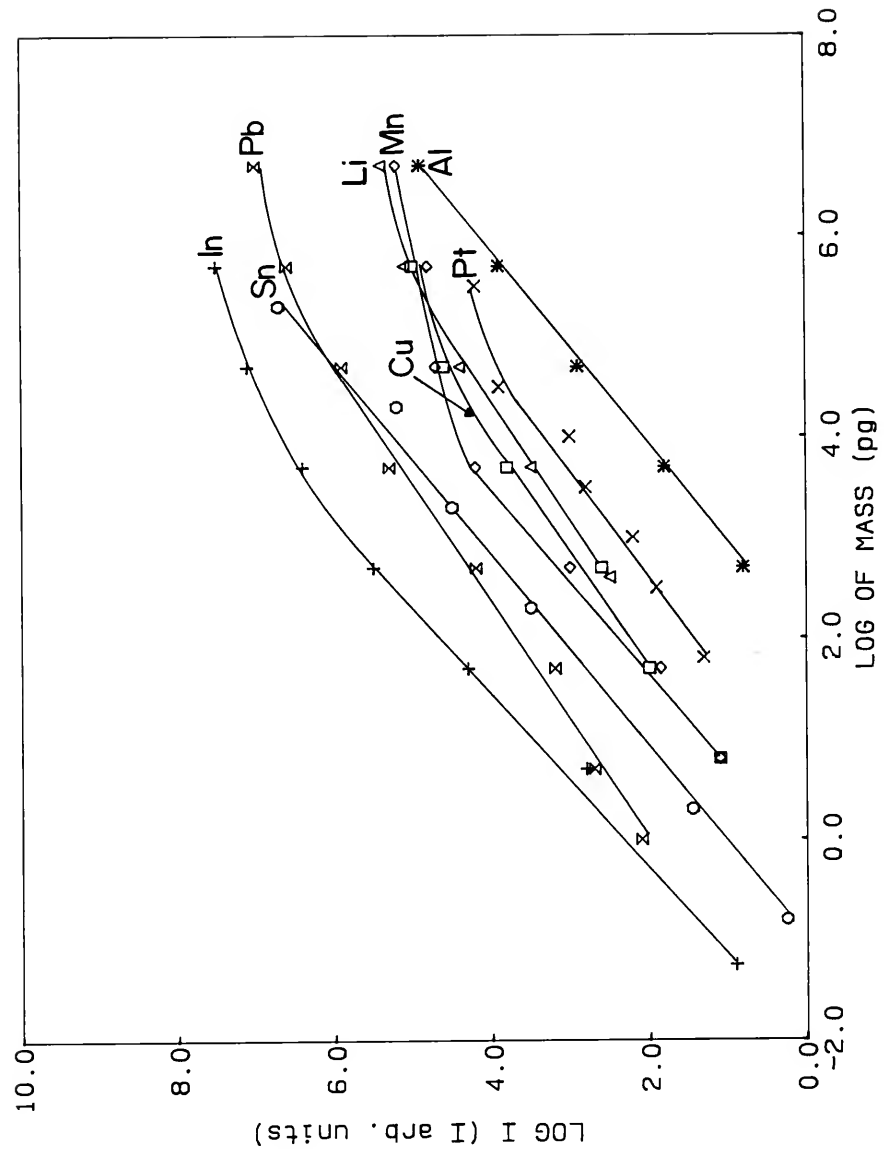
LOG I (I arb. units)
10.0
8.0
6.0
4.0
2.0
0.0
-2.0
0.0
2.0
4.0
6.0
8.0
LOG OF MASS (pg)
In
Pb
Sn
Li
Mn
Al
Cu
Pt

and fluorescence wavelengths. The improvements for Sn and In were also due to the hydrogen flame. Tin has previously been shown (55) to give improved detection limits when hydrogen was added to the argon sheath gas for atomic absorption spectrometry. Indium probably has improved detection limits due to its high volatility. Certainly, the cool hydrogen flame is hot enough to atomize In; keeping the In atoms in this atmosphere should minimize losses due to side reactions.

Copper and Mn have about an order of magnitude worse LODs than by previous fluorescence spectrometric studies. The poorer LODs were due to the close proximity of the excitation and fluorescence wavelengths. There was an increase in the magnitude of the scatter, and there was also an increase in the variability of scatter. The limiting noise here was a result of particles coming off of the graphite which flowed into the laser beam and scattered light into the monochromator. Although the pyrolytic coating improved detection limits and helped to protect the graphite surface, further improvements may have been found if the graphite had been pyrolytically coated by a commercial company; this would have insured the reproducibility of the coating from cup to cup. Another possible reason for the better LODs of Bolshov et al. (19) is that they used a Nd:YAG pump laser. This laser is capable of giving about an order of magnitude increased energy per pulse in the frequency-doubled range of the dye laser, when compared to the nitrogen laser as a pump source. The increased pulse energy should give an accordingly larger signal until saturation is achieved (1).

Lithium was the only element in which resonance fluorescence was used. The poor detection limit when compared to atomic absorption spectrometry is indicative of the scatter problems associated with resonance fluorescence. Lithium does not have a useful pair of excitation-emission lines that can be used for nonresonance fluorescence.

The poor detection limit for Pb was due to a large amount of contamination, both from the graphite cuvette and from the distilled-deionized water and reagents used to make up the standards. The low slope of the log-log calibration curve was due to a poor background correction. Even with the contamination, the detection limit was an improvement over the detection limit for atomic absorption spectrometry.

The aluminum LOD was two orders of magnitude worse than that for atomic absorption spectrometry. Part of the reason is due to the closeness of the excitation and fluorescence wavelengths as previously discussed. Another problem with Al is that it has a low volatility. The atomic absorption detection limits were carried out in a tube furnace, which provided much better atomization conditions, because of the semi-enclosed design. The fluorescence detection limits could be improved if the atomization was carried out in an enclosed furnace.

In general, the hydrogen flame acted only to provide a reducing atmosphere for the atomization process. Only in the case of In, which was very volatile, did the temperature of the hydrogen flame possibly help to atomize the sample.

CHAPTER 3
AN ENCLOSED FURNACE SYSTEM

The graphite furnace is generally surrounded by an argon atmosphere. The inert argon atmosphere keeps out contaminants from the air and also prevents the graphite from burning. Low pressure fluorescence (70,71) has also been utilized and it has resulted in the detection of individual atoms as they passed through a continuous wave laser beam by using a photomultiplier-photon counter system. This section describes an enclosed furnace system that was compatible with either an argon (Ar) atmosphere or a low pressure (LP) atmosphere.

The detection electronics were also changed at this time. The chart recorder was replaced by a personal computer (PC) as the readout for the fluorescence system. The benefits of this system will be discussed.

Experimental

Enclosed Furnace System

The laboratory built furnace (Figure 3-1) consisted of a phenolic base plate and a glass dome, which enclosed the copper electrodes and the graphite cup. The two copper electrodes were connected to the leads of the power supply by steel bolts that were fed through holes in the phenolic. A brass plate with an array of small holes was press fit into the center of the phenolic base. This plate allowed

Figure 3-1. Configuration of Furnace for Argon and Low Pressure Atmospheres.

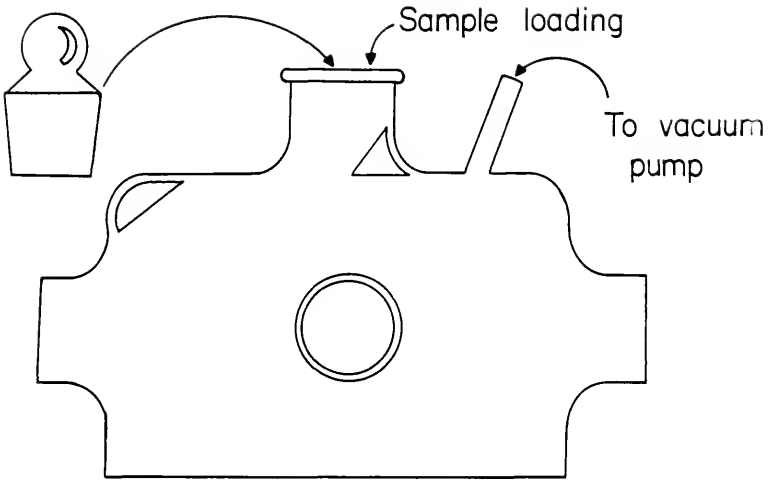
Sample loading
To vacuum pump

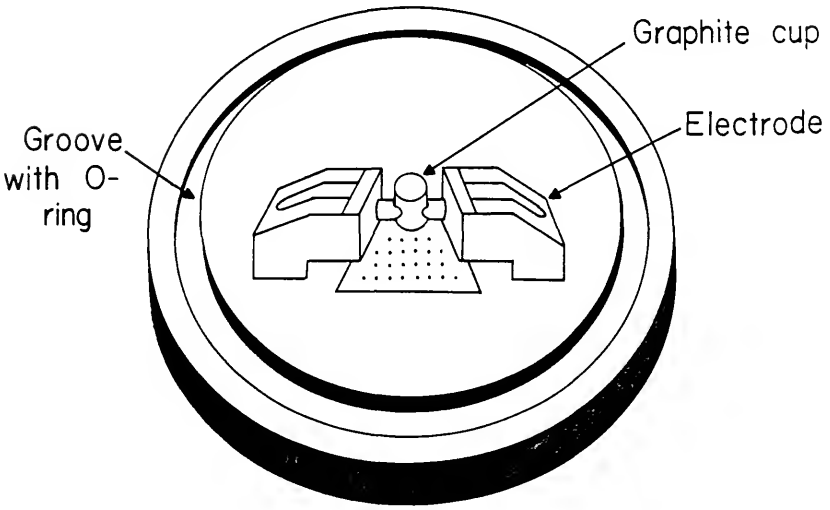
Graphite cup
Electrode
Groove with O-ring

argon to flow into the enclosure. Besides the benefits of the inert atmosphere, the argon also swept the atoms up into the laser beam. Two steel 1/4" tubes were also press fit through the phenolic to let in cooling water for the electrodes. A groove was cut into the phenolic surrounding the electrodes and water lines. Using vacuum grease, an o-ring in the groove formed a sufficient seal with the flat edge of the glass dome to allow a pressure down to 25 torr. Sealant was used around all of the fixtures (brass plate, electrodes, bolts, steel tubes) to keep air from entering the chamber. The glass top had three 1" quartz windows attached with epoxy. One window allowed the laser beam to enter while the opposite window allowed the laser beam to leave the enclosure. The exit window was used to minimize air entrainment and scatter from the glass dome (the curvature of the glass dome caused considerable scatter). There was also a quartz window at 90^{o} to these windows so that the fluorescence could pass through to the monochromator. There was a small outlet in the glass so that the Ar could escape; a Cajon connector was used to connect this outlet with a vacuum pump (Model 1400, General Electric, Skokie, IL) when the LP atmosphere was used. In this system, the laser was tuned using a nearby flame-monochromator system and the monochromator used with the furnace was tuned using a hollow cathode lamp.

Detection Electronics

The chart recorder used previously was replaced with a personal computer (Model 5150, IBM PC, Armonk, NY). Table 3-1 lists the equipment utilized. In order to make this change, a boxcar averager that was compatible with the computer system had to be used. The

Table 3-1
Equipment List of Modified Electronics System
Using the Enclosed Furnace System

Equipment	Manufacturer
SR 250 Boxcar Averager	Stanford Research Systems, 460 California Ave., Palo Alto, CA 94306
SR 225 Analog Processor	Stanford Research Systems, 460 California Ave., Palo Alto, CA 94306
SR 245 Computer Interface	Stanford Research Systems, 460 California Ave., Palo Alto, CA 94306
Model 4163 Preamplifier	Evans Associates, P.O. Box 5055, Berkeley, CA 94705
Model 5150 Personal Computer	IBM Corporation, Old Orchard Rd., Armonk, NY 10504

boxcar averager (SR 250, Stanford Research Systems), analog processor (SR 225, Stanford Research Systems), and computer interface (SR 245, Stanford Research Systems) were designed to be compatible with the IBM PC. A preamplifier (Model 4163, Evans Associates, Berkeley, CA) was used just before the boxcar averager to provide gain and to act as a filter.

The data acquisition program (SR 265, Stanford Research Systems) controlled both data acquisition and data reduction. The computer scan was started just prior to the atomization cycle and was stopped (manually) after the signal was completed. The computer allocated a position in memory (bin) every time the system received a trigger pulse (one trigger pulse for each laser shot). The system was synchronized by connecting the "Busy Output" of the boxcar averager to the "Sync" on the computer interface. The "Busy Output" provided a TTL synchronizing pulse when the unit was triggered. In this manner, a real time output was given by the computer. The integrals of the peaks were used as the measurement method.

Standard Reference Materials

In order to demonstrate the feasibility of this technique, the standard reference materials (SRMs) wheat flour (SRM 1567), spinach (SRM 1570), and steel (SRM 364) were determined for Cu and Mn.

All three samples were placed in a desiccator for 48 hours prior to weighing out any sample. After drying, the samples were weighed out above a given minimum sample size for each particular sample. The specified sample size was to insure homogeneity.

The dissolution technique (S. Hanomura, private communication, 1986) for the wheat flour and spinach consisted of placing each sample in a round-bottomed (RB) flask. Nineteen milliliters of purified nitric acid and 1 mL of sulfuric acid were added to the flask. The distilling apparatus included a nitric acid preserver, which consisted of a sidearm fitted with a stopcock. Gentle heating evaporated the nitric acid up into the condensing apparatus. As the nitric acid vapor recondensed, it would collect in the nitric acid preserver. When all of the nitric acid had evaporated out of the RB-flask, the heat would be turned off for 1 min, and then the nitric acid would be allowed to slowly drain from the nitric acid preserver back into the RB flask. The entire process would then be repeated. After several hours, the solution became clear. At this point, the dissolution was complete. The solution was transferred to a volumetric flask and then diluted up to 50 mL. The steel sample was put into solution by placing it in 30 mL of nitric acid along with 2 mL of sulfuric acid. The solutions were diluted up to 250 mL. Further dilutions were carried out as needed to bring the concentrations to a workable level.

Procedure

For the Ar atmosphere the procedure was the same as that for the H_2-Ar atmosphere. The argon flow rate was 5 L/min. For the LP atmosphere, the sample was dried at atmospheric pressure while argon was flowing through the enclosure. The argon was turned off and the enclosure was pumped down to 25 torr. The sample was then atomized as before. The SRM samples were determined in the Ar atmosphere. For

these samples, a charring step was included with temperatures of 500°C for Mn and 600°C for Cu.

Benefits of Computer System

The major advantage of using the computer for data reduction was that real time outputs were obtained. The data reduction routines allowed smoothing and background subtraction before measuring the integrals of the peaks. L'vov (44) emphasized the importance of correlating the integrated absorbance reading (rather than peak absorbance) with concentration. A matrix can cause the peak to become shorter and broader, causing erroneous measurements for the peak height method but leaving the integral the same. Also, refractory elements, such as Mo and V, tend to have severe tailing of the peak. An improved signal would result by using the integral method.

Figure 3-2 shows a printout of one of the peaks for In in an Ar atmosphere. If several more features were added, the computer could be used for determining the mechanistic pathway for the atomization (37,38). One feature that was added later was a spike in the printout that occurred at the beginning of the atomization cycle. In this manner, one could measure how long after the heating ramp started before the signal began (atomization time). By also adding in a temperature measuring system (using a calibrated photodiode) for the graphite cup, the atomization temperature could also be determined. These values could then be used to indicate the mechanistic pathway for atomization. The temperature feedback system would also help in assuring the reproducible heating of the furnace. The temperature

Figure 3-2. Printout of In Peak Atomized in the Argon Atmosphere. 1 bin α 33 ms. Note: The time shown prior to the peak is arbitrary and is not indicative of the atomization time.

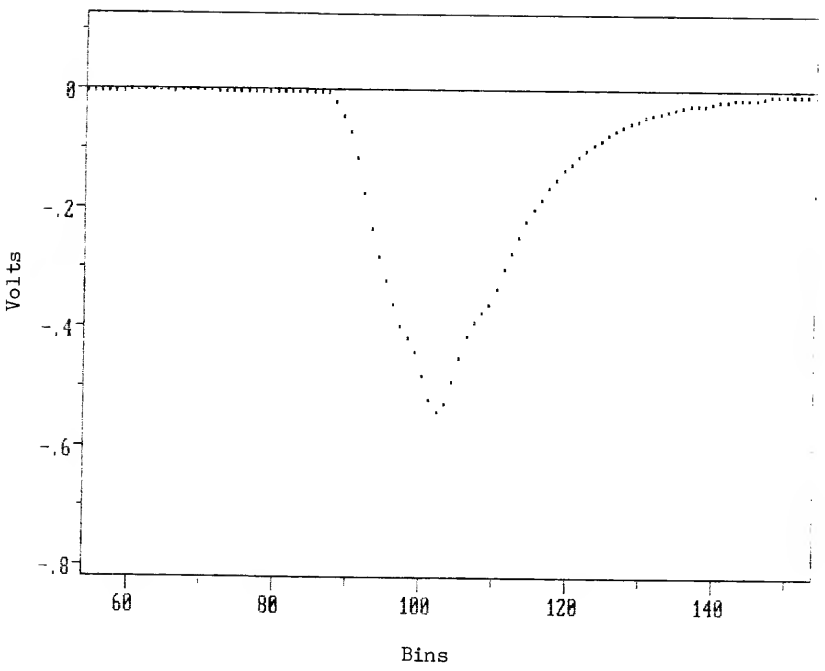
0
-.2
-.4
-.6
-.8
Volts
60
80
100
120
140
Bins

feedback system was not added due to time constraints and also because the research was moving in a different direction.

Results and Discussion

Comparison of Atmospheres

Figures 3-3 and 3-4 show printouts of the peak shapes for the H_2-Ar and LP atmospheres, respectively. There was a slight difference in the peak shape of the H_2-Ar atmosphere and the other two atmospheres. The ignition of the hydrogen may have caused the atomization to go to completion much faster (from the beginning of the peak to the maximum peak height). Suzuki et al. (81) suggested that the atomization mechanism may be altered in the presence of hydrogen. More information, such as the atomization temperature, would be needed to confirm this fact.

The results with H_2-Ar and LP atmospheres are compared in Table 3-2. The log-log calibration curves for the Ar and LP atmospheres are shown in Figures 3-5 and 3-6, respectively. In general, the LODs for the low pressure atmosphere were poorer than for the other two atmospheres. The original hope in carrying out this low pressure work was that the quantum efficiency for the fluorescence would be drastically improved because there would be no interferents to react with the atoms. Unfortunately, any improvement in quantum efficiency that may have occurred was more than nullified by the increased diffusion rates of the atoms. At low pressures, the atoms have high diffusion rates because there are few collisions with the inert gas. Since the atoms were in the path of the laser beam a shorter period of

Figure 3-3. Printout of In Peak Atomized in the H_2-Ar Atmosphere. 1 bin α 33 ms. Note: The time shown prior to the peak is arbitrary and is not indicative of the atomization time.

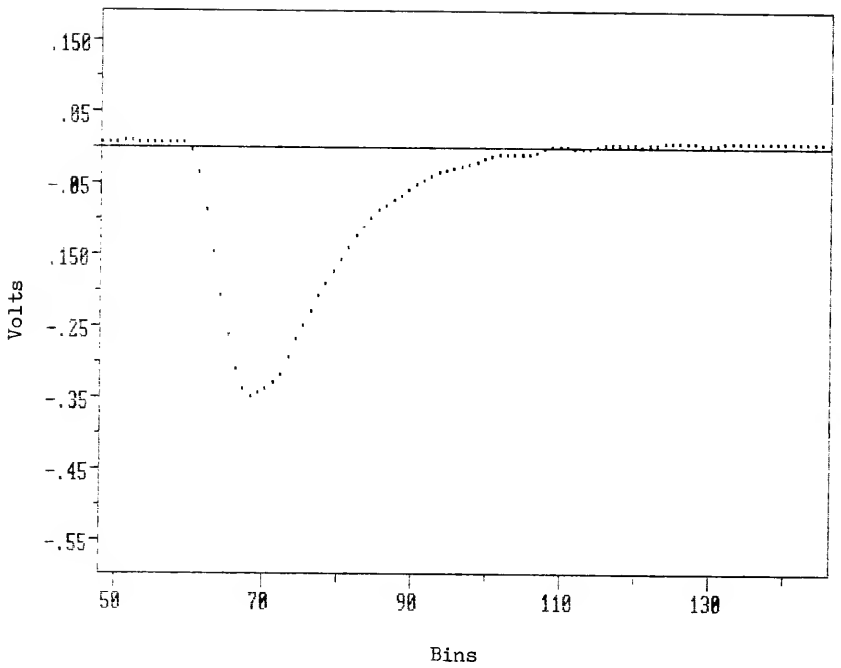
.150
.85
-.85
.150
-.25
-.35
-.45
-.55
Volts
50
70
90
110
130
Bins

Figure 3-4. Printout of In Peak Atomized in the Low Pressure Atmosphere. 1 bin ≈ 33 ms. Note: The time shown prior to the peak is arbitrary and is not indicative of the atomization time.

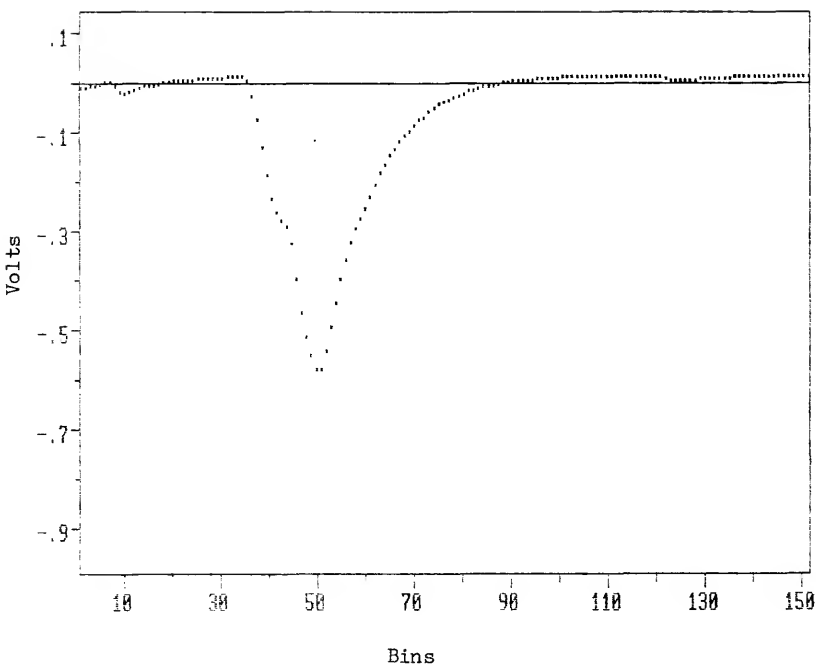
.1
-.1
-.3
-.5
-.7
-.9
Volts
10
30
50
70
90
110
130
150
Bins

Table 3-2
Comparison of Hydrogen-Argon (H_2-Ar), Argon (Ar), and Low Pressure (LP) Atmospheres (5 µL aliquots)

	Limits of Detection[a]			AUR[b]			Slope[c]		
	H_2-Ar	Ar	LP	H_2-AR	Ar	LP	H_2-Ar	Ar	LP
Cu	$7.X10^{0}$	$2.X10^{0}$	$2.X10^{2}$	4.5	5	3	0.91	1.05	0.95
Mn	$7.X10^{0}$	$1.X10^{0}$	$7.X10^{0}$	3	4	3	0.98	0.98	1.05
Pt	$6.X10^{1}$	$1.X10^{0}$	$2.X10^{1}$	3	3.5	>5	0.93	1.05	0.90
Sn	$2.X10^{-1}$	$1.X10^{1}$	-	>6	5	-	1.00	0.95	-
In	$5.X10^{-2}$	$3.X10^{-1}$	$7.X10^{-1}$	6	6	5	1.10	0.91	1.50
Li	$4.X10^{2}$	$4.X10^{2}$	$4.X10^{3}$	3	3	2.5	0.90	0.92	0.62

[a](pg), 3 σ/m, where σ = standard deviation of the blank and m = slope of calibration curve.

[b]Analytically Useful Range (orders of magnitude).

[c]Slope of log signal vs. log mass calibration curve.

Figure 3-5. Log Intensity vs. Log Mass for Elements Measured in an Ar Atmosphere. Slopes: Cu = 1.05, Mn = 0.98, Pt = 1.05, Sn = 0.95, In = 0.91, Li = 0.92. Typical RSD for each point is 10%.

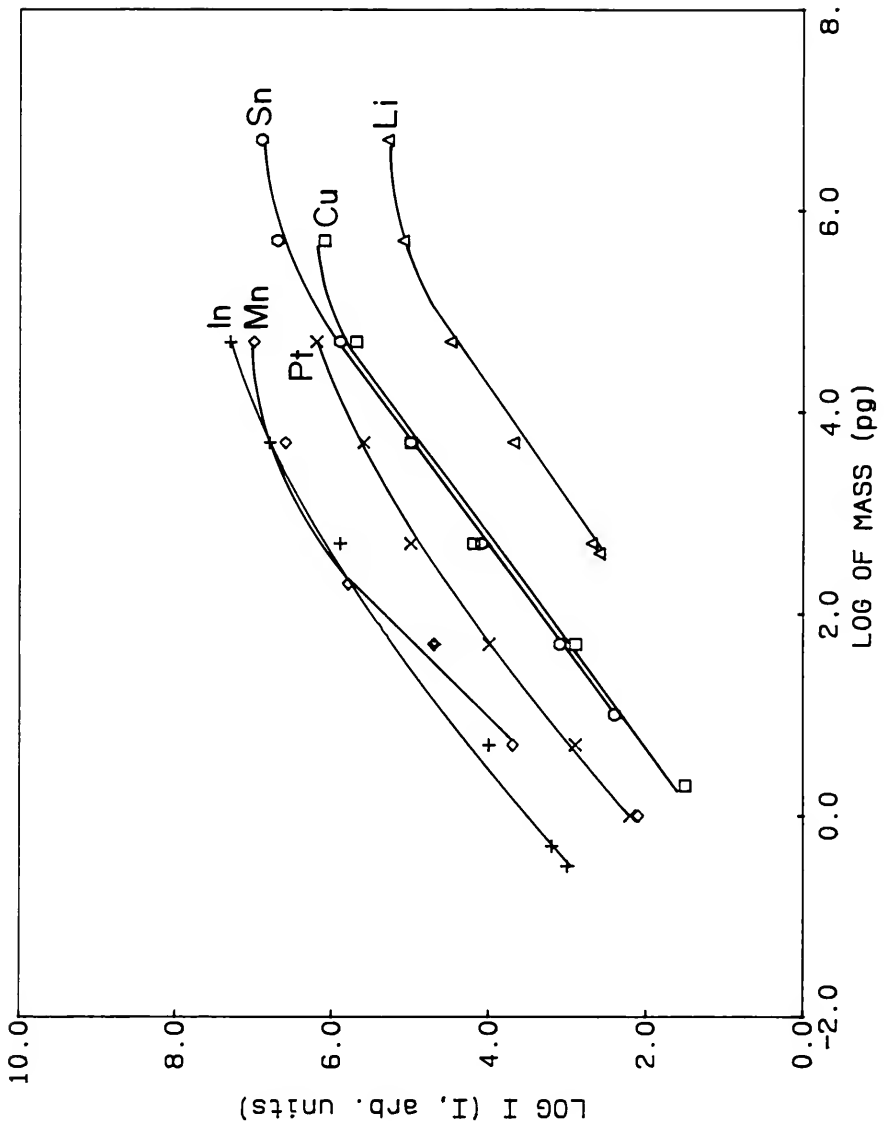
LOG I (I, arb. units)
10.0
8.0
6.0
4.0
2.0
0.0
-2.0
0.0
2.0
4.0
6.0
8.0
LOG OF MASS (pg)
In
Mn
Pt
Sn
Cu
Li

Figure 3-6. Log Intensity vs. Log Mass for Elements Measured in a Low Pressure Atmosphere. Slopes: Cu = 0.95, Mn = 1.05, Pt = 0.90, In = 1.50, Li = 0.62. Typical RSD for each point is 10%.

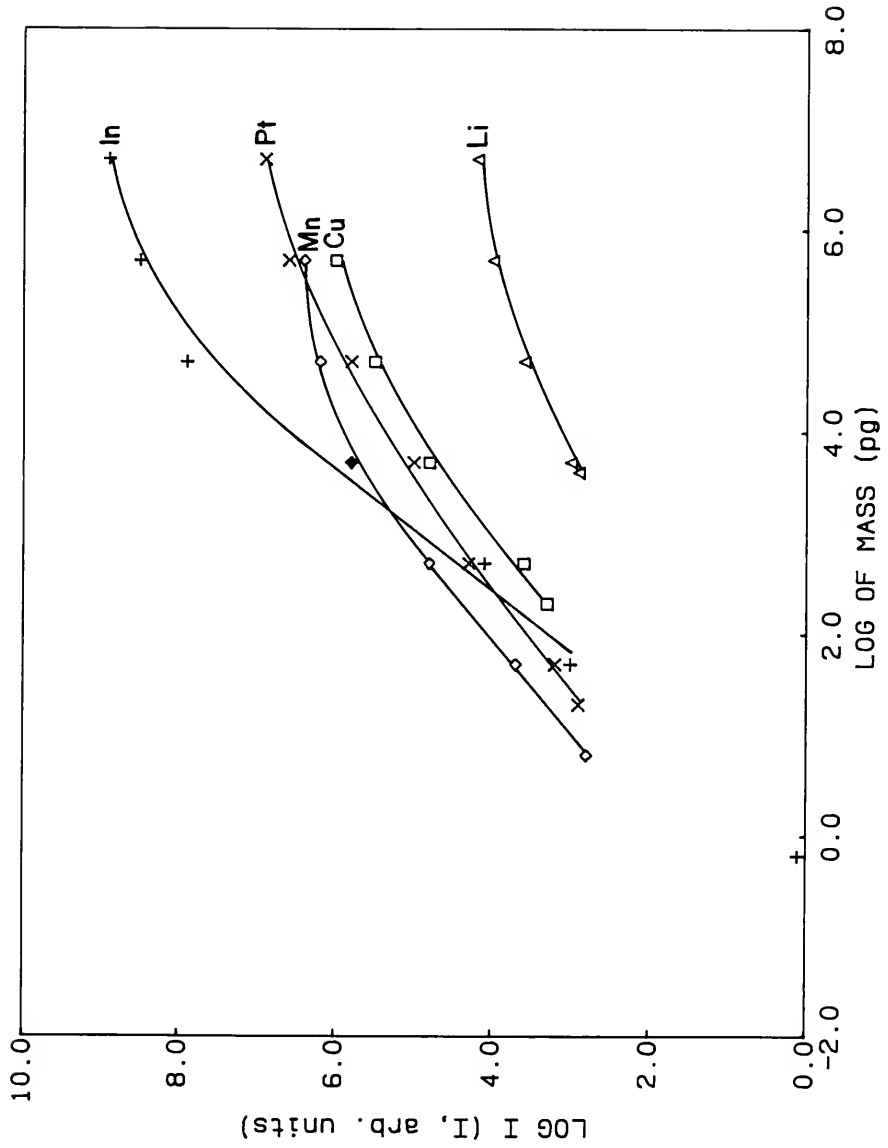
In
Pt
Mn
Cu
Li
LOG I (I, arb. units)
LOG OF MASS (pg)
10.0
8.0
6.0
4.0
2.0
0.0
-2.0
0.0
2.0
4.0
6.0
8.0

time and because of the relatively slow repetition rate of the laser, there was a decrease in signal.

An anomalous result occurred for Sn which gave no signal under low pressure except at 5000 ng, the highest amount used. This probably occurred due to the alteration of the mechanism of atomization; Rayson and Holcombe (55) suggested that oxygen attenuated the Sn signal by reacting with the Sn when measurements are at atmospheric pressure. However, at this time, there is not a good explanation for the loss in signal at low pressures.

The slopes of the log-log calibration curves for In and Li were also not unity, i.e., signal is $\alpha\ c^x$ when x=1 is considered a linear calibration. The low slope (0.62) for Li at LP is probably due to poor background correction caused by scatter. The low pressure apparently magnified this effect.

The reason for the extraordinarily high slope for In (1.50) at LP is not well understood. Sturgeon and Chakrabarti (38) have shown that the atomization time can change with pressure. However, at a particular pressure, the atomization time as well as the transport of the atoms into the laser beam should remain constant. There is no apparent reason why the signal should increase so disproportionately with analyte concentration.

The LODs in the H_2-Ar atmosphere and the Ar atmosphere were similar. The detection limits for Cu, Mn, and Pt were improved in the Ar atmosphere. Although the hydrogen flame provided a reducing atmosphere, the entire system was still open to the air.

Interferents, such as O_2, may have gotten through the argon sheath and the hydrogen flame to react with the atoms, causing losses. The enclosed Ar atmosphere was much easier to control and much more reproducible. The reasons for the excellent detection limits for Sn and In in the H_2-Ar atmosphere have previously been discussed.

SRM Results

The results from the SRM samples are shown in Table 3-3. The results were good considering the SRM samples were determined with aqueous standards. One of the benefits of atomic fluorescence over atomic absorption is that in many cases accurate results can be obtained without having to make standards in a matched matrix.

Comparison With Previous Studies

In Table 3-4, LODs obtained in this work are compared with other literature values for the same technique and also furnace atomic absorption spectrometry. The LODs for Sn and Pt in the H_2-Ar and Ar atmospheres, respectively, are considerably improved over the previous results, while the In LODs are slightly improved.

These results show that both the H_2-Ar and Ar atmospheres work very well. The best results occurred for elements with a relatively large separation in their excitation and fluorescence wavelengths. Also, the more volatile elements tended to give better results. The Al results suggest that an enclosed furnace was needed to improve the atomization efficiency of nonvolatile elements.

Table 3-3
SRM Standards (ppm, except where noted)

		Mn		Cu	
Sample	NBS#	Expt.	Given	Expt.	Given
Wheat Flour	1567	7.3±0.8	8.5±0.5	2.5±0.1	2.0±0.3
Spinach	1570	128±9	165±6	17±2	12±2
Steel	364	0.23%	0.25%	0.29%	0.24%

Table 3-4
Limits of Detection (pg) by Laser-Excited Atomic Fluorescence in a Graphite Furnace (5 μL aliquots)

Element	Wavelength (nm)		LAFS[a]				GFAAS[c]
	Exc.	Fl.	H_2-Ar	Ar	LP	Lit.[b]	
Cu	324.8	327.4	$7.X10^{0}$	$2.X10^{0}$	$2.X10^{2}$	$2.X10^{-1}$	$2.X10^{0}$
Mn	279.8	280.1	$7.X10^{0}$	$1.X10^{0}$	$7.X10^{0}$	$2.X10^{-1}$	$4.X10^{-1}$
Pt	265.9	270.2	$6.X10^{1}$	$1.X10^{0}$	$2.X10^{1}$	$1.X10^{2}$	$2.X10^{1}$
Sn	286.3	317.5	$2.X10^{-1}$	$1.X10^{1}$	-	$5.X10^{2}$	$2.X10^{1}$
In	303.9	325.6	$5.X10^{-2}$	$3.X10^{-1}$	$7.X10^{-1}$	$1.X10^{-1}$	NR[d]
Li	670.8	670.8	$4.X10^{2}$	$4.X10^{2}$	$4.X10^{3}$	NR[d]	$3.X10^{1}$
Pb	283.3	405.8	$2.X10^{-1}$	-	-	$2.X10^{-3}$	$5.X10^{0}$
Al	394.4	396.2	$5.X10^{2}$	-	-	NR[e]	$1.X10^{0}$

[a]Laser-excited atomic fluorescence with a graphite furnace. Limit of detection is defined as 3 σ/m, where σ = standard deviation of the blank and m = slope of calibration curves.

[b]Data for In and Sn from (23); Pb, Mn, Cu, and Pt from (19).

[c]Data from (80).

[d]NR = No Report.

CHAPTER 4
A GRAPHITE TUBE FURNACE FOR LASER-EXCITED ATOMIC FLUORESCENCE

In most of the atomic fluorescence works utilizing a graphite furnace, an open furnace (15-24), such as a graphite cup, has been used. A tube furnace has been utilized most often in atomic absorption spectrometry. The semi-enclosed design of the tube provides better conditions for atomization than does the graphite cup. The difficulty with using a tube furnace for atomic fluorescence is viewing the fluorescence at 90°. Dittrich and Stark (25) observed fluorescence using holes in the sides of a graphite tube to send the laser beam through and then viewing the fluorescence through the end of the tube. However, they only reported improved sensitivities (slope of calibration curve) and did not discuss any other figures of merit.

Because of the poorer atomization conditions of the graphite cup, many of the refractory elements have not been studied by atomic fluorescence using a graphite furnace. The refractory elements generally require very high temperatures for atomization due to the formation of involatile carbides with the graphite (41-43). In Chapter 2, poor results were obtained for Al when using the graphite cup. In order to improve on those results, better atomization conditions were needed. This section describes a tube furnace to be used with laser-excited atomic fluorescence.

Experimental

Figure 4-1 shows the layout of the tube furnace system. The laser beam passed through a hole (1/4") in the mirror and then excited the atoms in the graphite tube. The fluorescence was collected back in the same direction as the laser beam. The fluorescence was reflected off of the mirror and then a 1:1 image of the fluorescence was focused by a lens (2 in dia., 3 in F.L.) into the monochromator. The tube furnace was placed in the enclosed Ar atmosphere; there was a glass dome over the tube furnace and both the laser beam and the fluorescence had to pass through a quartz window. The quartz window was between the tube furnace and the mirror. One change made to this quartz window was that the glass arm holding the window was cut at a 45° angle upward. Consequently, the small (~5%) laser reflection from the window was directed upward rather than back towards the mirror where it might be directed into the monochromator, causing a large scatter signal. The graphite tube (Figure 4-2) was held between two spring-loaded graphite electrodes. The graphite tube was not pyrolytically coated due to excessive heat from the bulky tube furnace during pyrolysis; the pyrolysis chamber could not withstand this heat. Two power supplies (TCR 3ϕ, Electronics Measurements, Neptune, NJ) were wired in parallel to provide rapid heating of the graphite tube. The same controlling circuit (Chapter 2) was used for controlling these power supplies. The laser system, the Ar furnace system, and the detection electronics were the same as described in Chapter 3.

Figure 4-1. Optical Layout of Tube Furnace System for Laser-Excited Atomic Fluorescence.

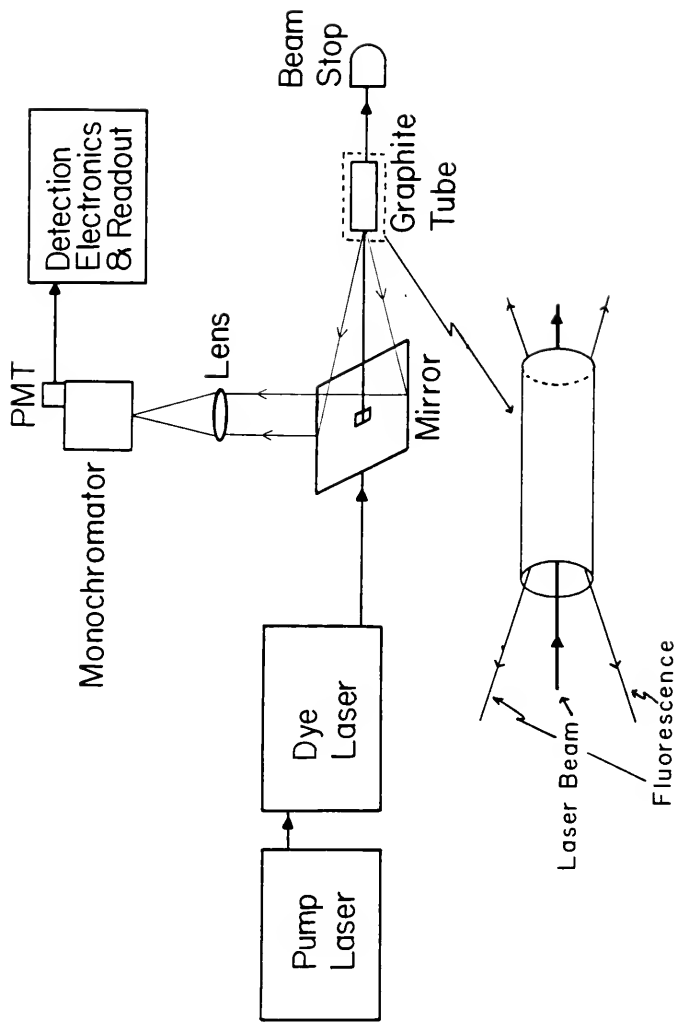
Pump Laser
Dye Laser
Monochromator
PMT
Detection Electronics & Readout
Lens
Mirror
Beam Stop
Graphite Tube
Laser Beam
Fluorescence

Figure 4-2. A Graphite Tube Furnace for Laser-Excited Atomic Fluorescence.

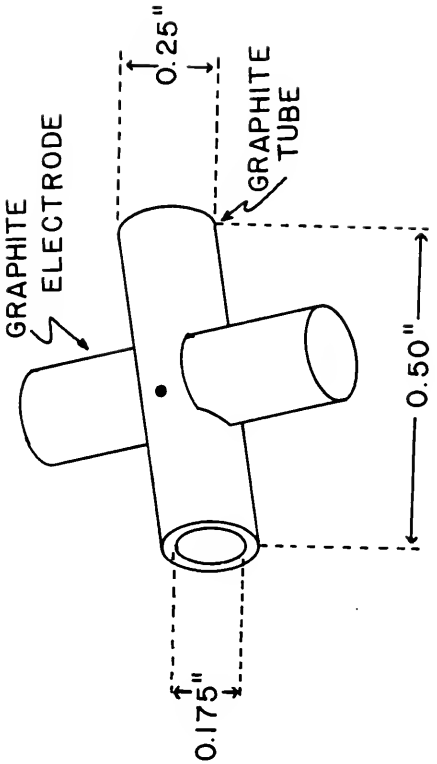
GRAPHITE
ELECTRODE
0.25"
GRAPHITE
TUBE
0.50"
0.175"

The mirror and graphite tube system were lined up by placing the mirror in such a way that the laser beam would pass through the hole in the mirror and also the graphite tube. The monochromator was set in the visible wavelength region and the output from the photomultiplier tube was connected directly to a chart recorder. The graphite tube was then heated for a long period of time while the mirror and lens were aligned to give the largest signal from the graphite emission. This alignment insured that the center of the graphite tube was focused onto the monochromator slit.

Results and Discussion

Table 4-1 lists the results for the tube furnace. Figure 4-3 shows the calibration curves for the elements measured. In comparing these results with the previous graphite cup results, the detection limit for Cu was poorer and for Al was better. Also, it should be noted Mo and V were not even measurable in the graphite cup, but were detectable in the tube furnace, which shows an improvement for the latter.

The Cu results were slightly worse in the tube furnace than for the cup furnace because Cu is relatively volatile and therefore atomizes easily in the graphite cup. When using the graphite tube, the amount of fluorescence collected was significantly less than with the cup furnace. In the tube furnace there were light losses when fluorescence escaped through the hole in the mirror which allowed the laser to pass through. Also, the graphite tube limited the solid angle of light exiting the tube. For these reasons, the tube furnace

Table 4-1
Limits of Detection (pg) for
the Tube Furnace (5 μL aliquots)

Element	Wavelength (nm)		This Work[a]		GFAAS
	Exc.	Fl.	Tube	Cup	
Al	394.4	396.2	$1.X10^{2}$	$5.X10^{2}$[b]	$1.X10^{0}$
Cu	324.8	327.4	$8.X10^{0}$	$2.X10^{0}$	$2.X10^{0}$
Mo	313.3	317.0	$1.X10^{2}$	NS[c]	$1.X10^{2}$
V	385.6	411.2	$2.X10^{5}$	NS[c]	$2.X10^{1}$

[a]Limit of detection is defined as $3\ \sigma/m$, where σ = standard deviation of the blank and m = slope of calibration curve.

[b]Hydrogen-argon atmosphere.

[c]NS = No Signal.

Figure 4-3. Log Intensity vs. Log Mass for the Graphite Tube Furnace. Slopes: Cu = 0.90, Mo = 0.80, Al = 0.55, V = 0.95. Typical RSD for each point is 10%.

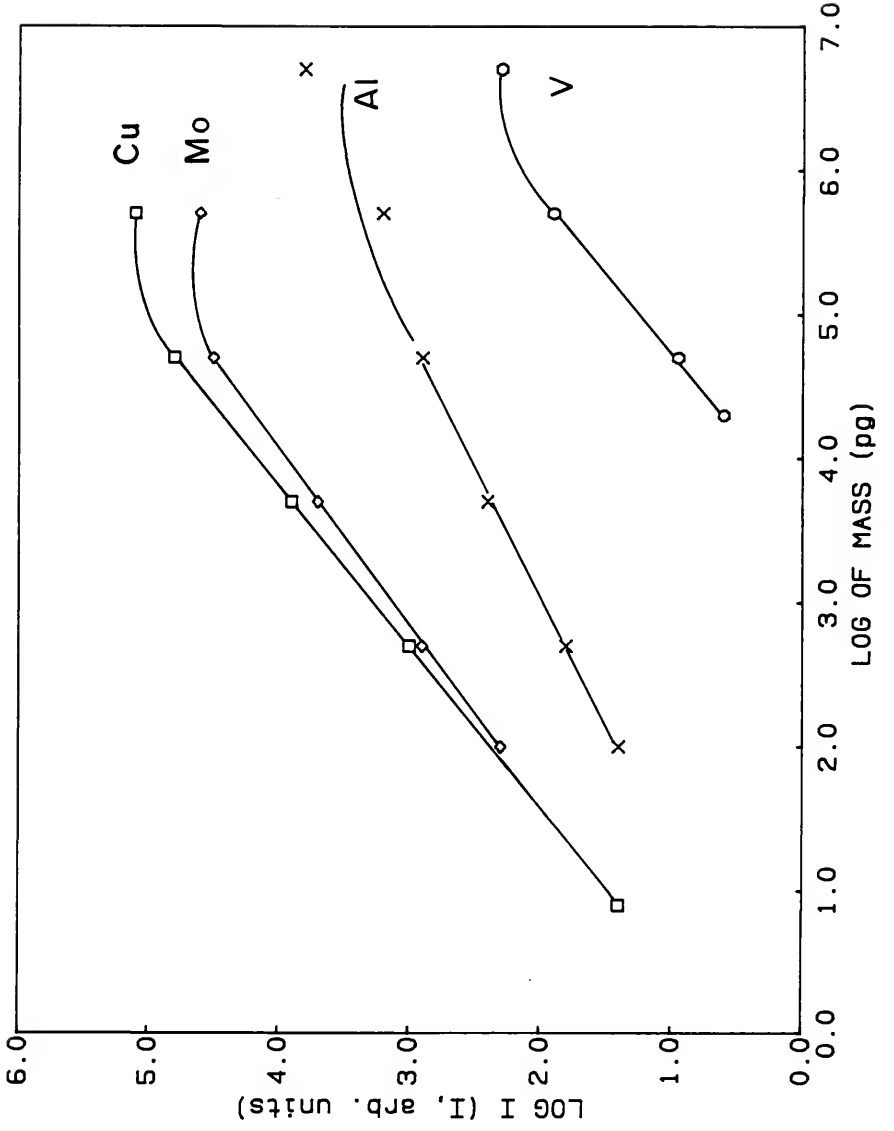
Cu
Mo
Al
V
LOG I (I, arb. units)
LOG OF MASS (pg)
0.0
1.0
2.0
3.0
4.0
5.0
6.0
7.0

did not work as well as the plain graphite cup for the more volatile elements.

The improved results for Al, Mo, and V showed that the graphite tube was more effective in atomizing these elements than the graphite cup. The semi-enclosed furnace was necessary for atomizing these refractory elements (Mo, V).

The results were still significantly worse than the values for atomic absorption, especially for V. The results from this work could have been greatly improved if a pyrolytic coating for the graphite had been used. The pyrolytic coating helps to minimize carbide formation. Also, the limiting noise on the blank was laser scatter into the monochromator from particles ejected from the graphite surface. The pyrolytic coating would have minimized most of this scatter. Another problem was the laser scatter caused by the front quartz window. Even though most of the scatter was deflected upward, a small portion would still be measured by the photomultiplier tube. In most cases, at least a "2" (orders of magnitude) neutral density filter had to be used in front of the monochromator so that the detection electronics would not be overloaded. By placing the front quartz window at the Brewster angle (82), such scatter would have been minimized.

The other major problem was light losses through the hole drilled in the mirror. A 1/8" hole was originally used but alignment was much more difficult, and there was more scatter as the laser beam passed through the hole. This scatter was worse when a frequency-doubled beam was used since this beam had a much larger diameter.

Even with the problems associated with viewing the fluorescence at 90°, better LODs were obtained for nonvolatile elements using the tube furnace. The more volatile elements worked better with the plain graphite cup.

CHAPTER 5
THE COPPER VAPOR LASER AS A PUMP LASER

Laser-excited atomic fluorescence with a graphite furnace has generally employed either a nitrogen laser (17,21,23,25), an excimer laser (22), or a Nd:YAG laser (16,18-20) as the pump laser. All of these lasers have very high energies/pulse (e.g., 10 mJ/pulse for a N_2 laser) and broad tuning ranges when used with a dye laser (360-900 nm in the fundamental and 220-360 nm in the frequency-doubled range). For the most part, they can only be operated on the order of 50 Hz or less. In most applications, this repetition rate is quite adequate. When using a graphite furnace though, the atomic vapor emerging from the furnace is in the path of the laser for only about 2 s at most. Because the pulse widths of these lasers are on the order of 10 ns and because of the slow repetition rate, many of the atoms escape without ever being excited by the laser. One possible solution to this problem is to use a copper vapor laser (CVL), which operates at 6 kHz.

The CVL was developed in 1966 (83) and is still somewhat of a novelty among scientists. The early lasers achieved only 20 mW average power and a lifetime of a few hours. Now, the CVL operates at average output powers of 10-40 W and lifetimes of several hundred hours (84), before reloading of Cu is necessary. Some of the possible

applications (85) of this laser are underwater research, photography and holography, semiconductor research, and fingerprint detection.

Comparison of a Nitrogen Laser and a CVL as a Pump Laser

Table 5-1 compares some important specifications for dye lasers when pumped either by a nitrogen laser or a CVL. The big advantage to using the CVL with a furnace is that this laser will produce 12,000 laser pulses while the analyte atomic vapor is present in the furnace (~2 s). With this many laser pulses, every atom should be excited many times. The CVL also had a longer pulse width, yielding a better possibility of exciting all of the atoms.

The major disadvantage of the CVL was the limited tuning range of the dye laser. The wavelengths of excitation for the CVL were 510 nm and 578 nm; therefore, the fundamental dye range was above these wavelengths. Even with frequency doubling, there was still a "hole" in the tuning range. There have only been a limited number of works (86-88) that have dealt with utilizing different dyes to extend the tuning range of the laser. This tuning range could easily be extended to longer wavelengths (e.g., 900 nm), but there would still be a "hole" in the tuning range.

Experimental

Copper Vapor Laser System

The laser system consisted of a CVL (Model 251, Plasma Kinetics, Pleasanton, CA) and a dye laser (DL 13, Molectron, Palo Alto, CA). The CVL was operated at 6 kHz. The only major differences between

Table 5-1
Comparison of Nitrogen and
Copper Vapor-Pumped Dye Lasers

Dye Laser Characteristics	Nitrogen Laser Pump	CVL Pump
Fundamental Tuning Range	360-950 nm	525-700 nm[a]
Frequency Doubled Range	217-360 nm	260-350 nm[b]
Pulse Width	5 ns	24-30 ns
Repetition Rate	0-50 Hz	6 kHz (nominal)
Pulse Energy	1 mJ	0.3 mJ
Peak Power	200 kW	15 kW

[a]Published data to date.

[b]Assumed values from fundamental tuning range.

this dye laser and the nitrogen-pumped dye laser were that the turning mirrors for the CVL-dye laser were coated to reflect the 510 nm and 578 nm wavelengths (rather than 337 nm) and the dye pump (Model DL-363, Molectron) had a much higher flow rate. The high flow rate was necessary to prevent heating of the dye caused by the high repetition rate of the CVL. Table 5-2 lists the dyes used for the CVL system. When dyes were used that lased below 578 nm, a dichroic mirror was used to block the 578 nm wavelength from the CVL.

The external frequency-doubling system (Autotracker II, INRAD, Northvale, NJ) was capable of tracking the fundamental wavelength so that the frequency-doubled power would stay optimized. A focusing lens (1 in dia., 4 in F.L.) was placed just prior to the frequency-doubling system. While the autotracking accessory was not necessary for data collection, it was very convenient for scanning the laser when trying to locate the excitation wavelength in the flame.

Because the CVL-dye laser system was at the opposite end of the laboratory from the furnace system, a 24-foot fiber optic cable (quartz, 600 μm core, Quartz and Silice, Plainfield, NJ) was used to send the dye laser beam down to the furnace system. A focusing lens (1.5 in dia., 3 in F.L.) was used to focus the beam into the fiber optic. On the furnace end, a focusing lens (1.5 in dia., 2 in F.L.) was used to project a nearly 1:1 image of the laser beam (as it exited the fiber optic) over the furnace. In practice, the lens was adjusted so that the laser beam was the same diameter as the graphite cup. An aperture was also used to reduce the stray light.

Table 5-2
Dye List for Copper Vapor-Pumped Dye Laser

Dye	Concentration (M)	Solvent	WL Range (nm)	Freq. Dbl. WL Range (nm)
Oxazine 720	$6.6X10^{-4}$	methanol	655-700	328-350
Rhodamine 6G + Kiton Red 620	$8.8X10^{-4}$ $2.1X10^{-4}$	methanol	575-614	288-307
Kiton Red 620	$1.7X10^{-3}$	methanol	588-639	294-319

Because of the limitation in the data transfer rate (1.4 kHz) to the computer (89), the computer was only triggered at one tenth the rate as compared to the boxcar averager and the laser. A decade counter (74LS90, Texas Instruments, Dallas, TX) was utilized to divide the frequency of the "Busy Output" (synchronization pulse) from the boxcar averager by ten. This lower frequency (600 Hz) was then used to trigger the computer. All data points were collected at the 6 kHz rate and averaged by the boxcar averager. The averaged output from the boxcar averager was sent to the computer at a rate of 600 Hz. In this manner, no data were lost.

The nitrogen-dye laser system was the same as that described in Chapter 2.

Procedure

The elements In, Li, and Na were each determined with both laser systems. The In was measured using the H_2-Ar atmosphere (but with the computer system as the detection electronics). The Li and Na were determined in the Ar atmosphere. All three elements were determined in the plain pyrolytic graphite cup. The CVL system was tuned to the particular elemental line by moving the end of the fiber optic over to the flame system used for tuning the nitrogen-dye laser system. A blade connected to a rotary solenoid motor was used to block the laser beam when loading samples into the graphite cup.

In order to excite Li at 671 nm, a dye had to be used with its maximum power near that wavelength. To help choose a dye, the dyes used for the Ar^+ laser (514 nm) and also the frequency-doubled output of the ND:YAG laser (532 nm) were investigated. Oxazine 720 appeared

promising; therefore, a $1X10^{-3}$ M solution was prepared and found to lase in the required wavelength region. The power at 671 nm was monitored while the dye was diluted; maximum power was achieved at a concentration of $6.6X10^{-4}$ M.

Results and Discussion

Figure 5-1 shows the lasing curve for the oxazine 720. The maximum output power was 0.76 W, which was approximately half of the power measured for rhodamine 6G at its peak. This power ratio was similar to power ratios obtained from other pump lasers (90). These results indicated that the oxazine 720 dye worked very well.

Problems Associated With the Fiber Optic

The main reason for having to use the fiber optic was because of space restrictions. Before using the fiber optic, the beam was directed down the laboratory using mirrors. Unfortunately, five mirrors had to be used to direct the beam around and above other equipment in the laboratory; also, the beam diverged to a diameter of 3 in by the time it arrived at the furnace. The beam divergence could have probably been dealt with using collimating lenses, but the main problem was the five mirrors. Not only were there light losses at each mirror, but lining up the laser each day became tedious and time consuming. There was also the safety problem of sending the laser beam down the length of the laboratory, even though safety shielding was put in place. Because of all of these reasons, the fiber optic approach was chosen as the only alternative.

Figure 5-1. Lasing Curve for Oxazine 720 ($6.6X10^{-4}$ M).

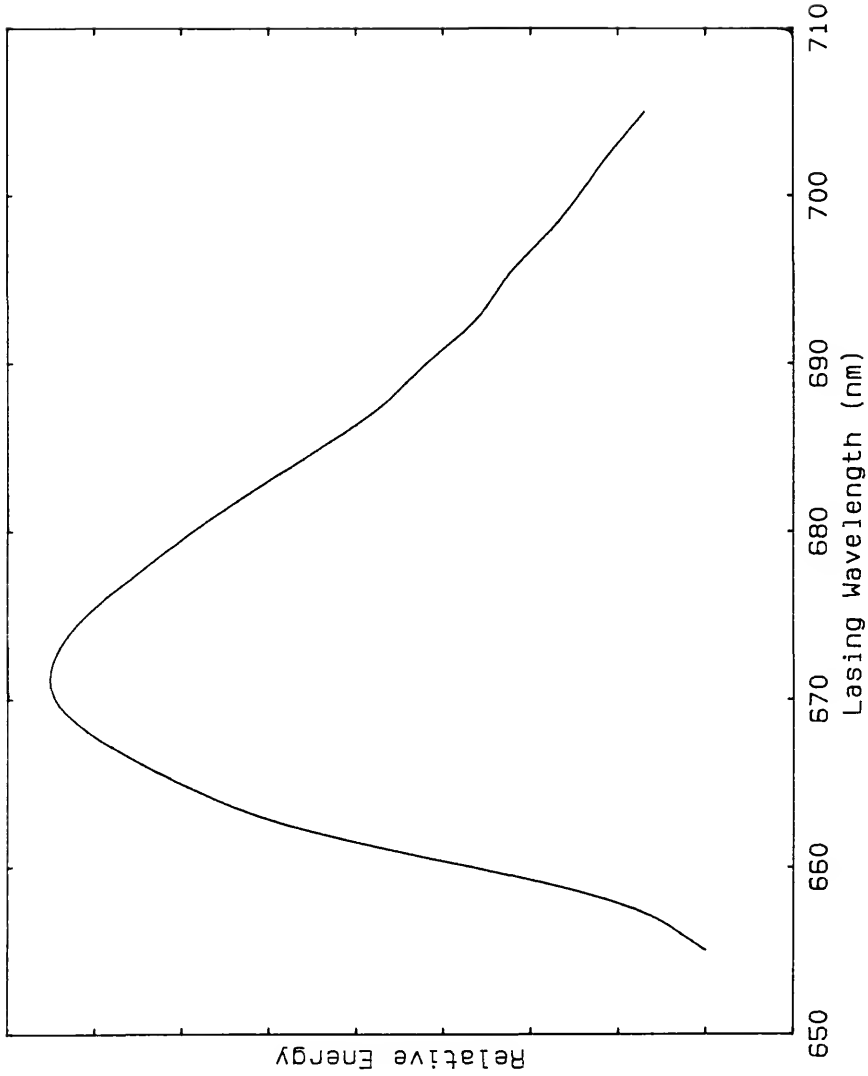
Relative Energy
650
660
670
680
690
700
710
Lasing Wavelength (nm)

For the ultraviolet (UV) laser beam, the efficiency of the fiber optic was 15% and for the visible laser wavelengths the efficiency was about 45%. These low efficiencies were still improved over sending the laser beam down the lab with mirrors. The poor efficiency of the fiber optic in the UV region was one of the contributing factors to deciding to determine elements in the visible region, after trying In (304 nm). The efficiencies may have been improved somewhat if a commercial coupler for the laser beam into the fiber optic had been used. The positioning mounts and lens system were certainly not up to the standards of a commercial coupler.

Comparison of Results

Figure 5-2 shows a printout of an In peak when using the CVL. The advantage of the high repetition rate is obvious because of the large number of laser pulses during the peak. Table 5-3 lists the LODs for the CVL and the nitrogen laser. Figures 5-3, 5-4, and 5-5 show the log-log calibration curves for In, Li, and Na, respectively.

The poor results obtained for In with the CVL were somewhat expected. The frequency-doubling efficiency was only about 2% for the CVL while the efficiency was about 5% for the nitrogen laser. The lower doubling efficiency was due to the low pulse energy of the CVL-dye laser system. This fact, coupled with the poor transmission quality of the fiber optic, led to the poor results for In.

The Li results suggested that the CVL can be an effective pump laser. The high repetition rate of the CVL provided a larger signal and therefore an improved detection limit. The low slopes for the

Figure 5-2. Printout of In Peak Using the CVL as the Pump Laser. 1 bin α 2 ms. Note: The time shown prior to the peak is arbitrary and is not indicative of the atomization time.

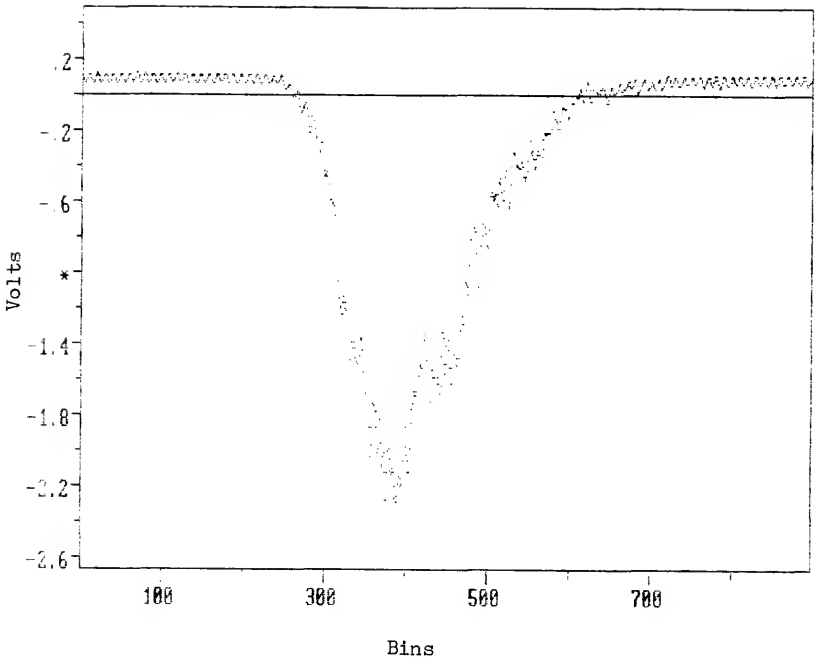
.2
-.2
-.6
*
-1.4
-1.8
-2.2
-2.6
Volts
100
300
500
700
Bins

Table 5-3
Limits of Detection for Copper Vapor
and Nitrogen-Pumped Dye Lasers

Element	Limit of Detection (pg)[a]--Pump Laser	
	Nitrogen	Copper Vapor
In	$6.X10^{-2}$	$4.X10^{-1}$
Li	$4.X10^{2}$	$6.X10^{1}$
Na	$8.X10^{-1}$	$1.X10^{0}$

[a]Based on 5 µl aliquots. Limit of detection is defined as 3 σ/m, where σ = standard deviation of blank and m = slope of calibration curve.

Figure 5-3. Log Intensity vs. Log Mass for In Using the N_2 Laser and CVL as Pump Lasers. Slopes: N_2 = 1.09, CVL = 1.12. Typical RSD for each point is 10%.

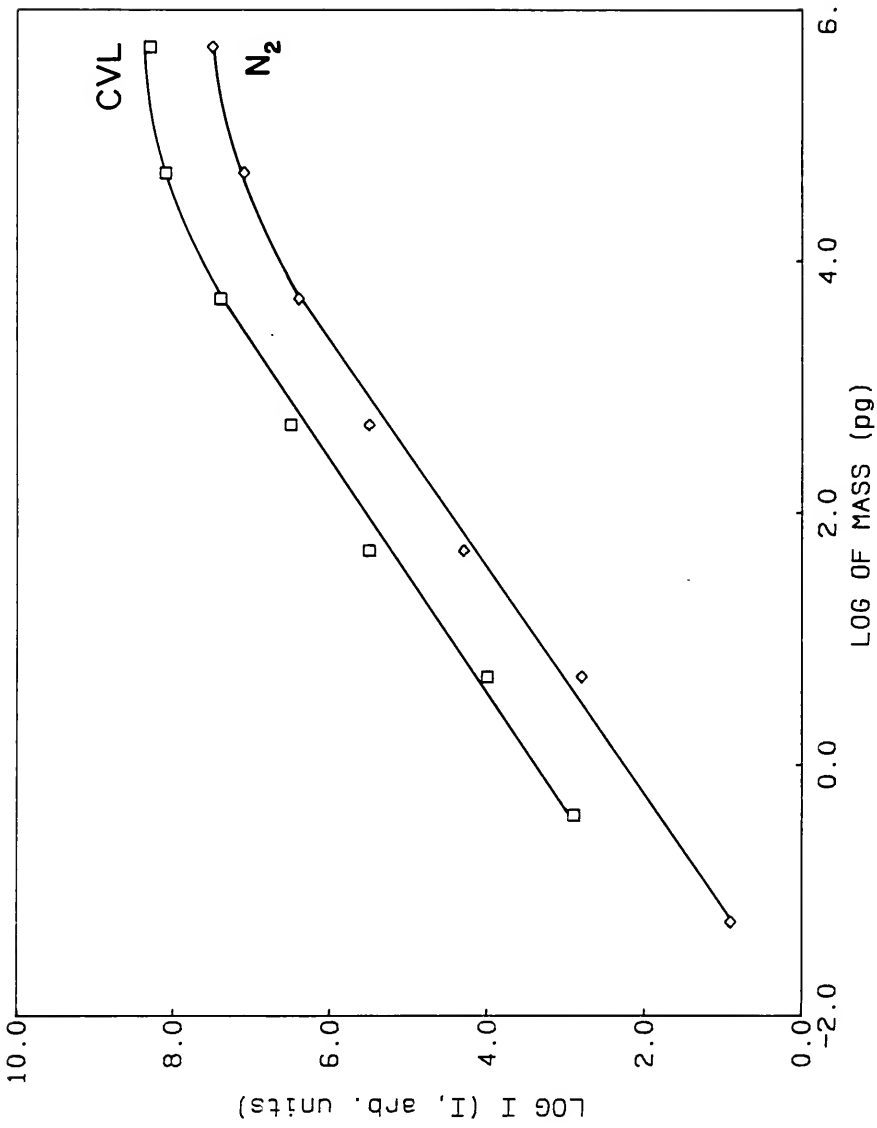
CVL
N_2
LOG I (I, arb. units)
LOG OF MASS (pg)
10.0
8.0
6.0
4.0
2.0
0.0
-2.0
0.0
2.0
4.0
6.0

Figure 5-4. Log Intensity vs. Log Mass for Li Using the N_2 Laser and CVL as Pump Lasers. Slopes: N_2 = 0.92, CVL = 0.90. Typical RSD for each point is 10%.

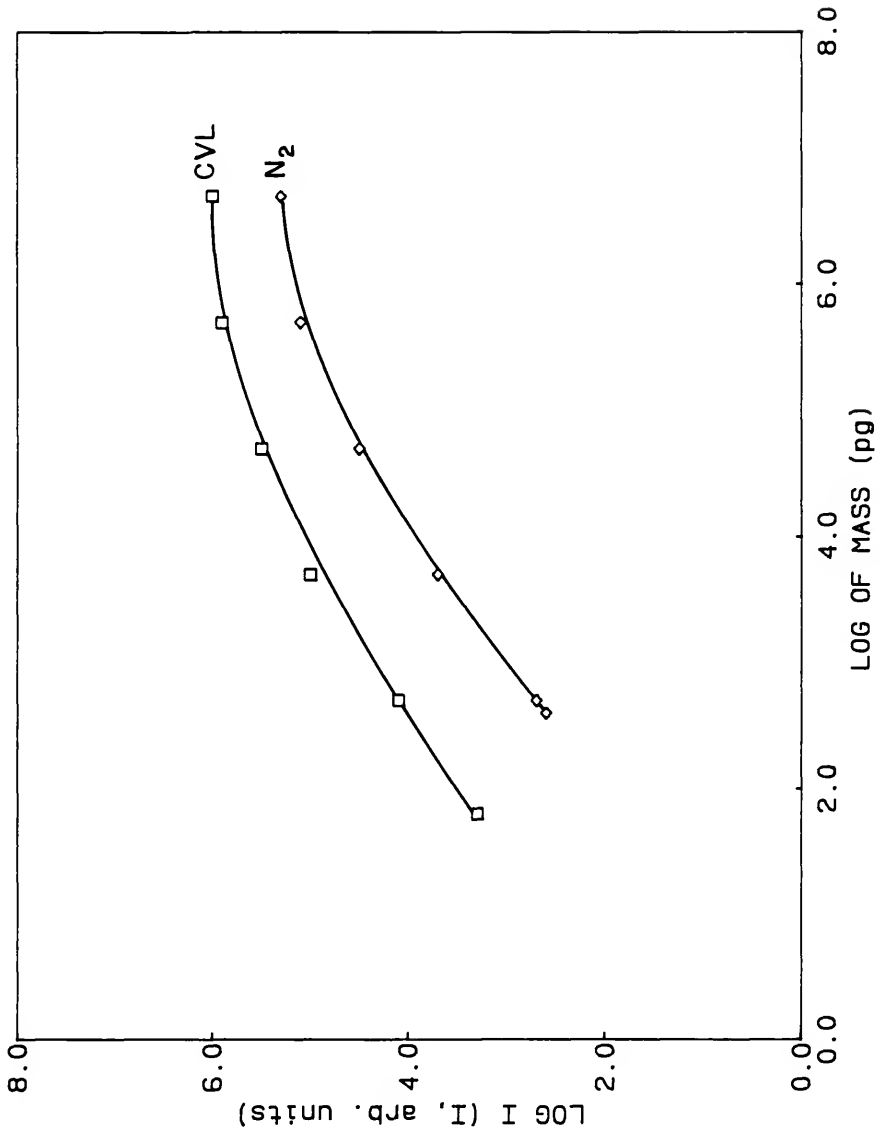
CVL
N_2
LOG I (I, arb. units)
LOG OF MASS (pg)
0.0
2.0
4.0
6.0
8.0

Figure 5-5. Log Intensity vs. Log Mass for Na Using the N_2 Laser and CVL as Pump Lasers. Slopes: N_2 = 1.20, CVL = 0.68. Typical RSD for each point is 10%.

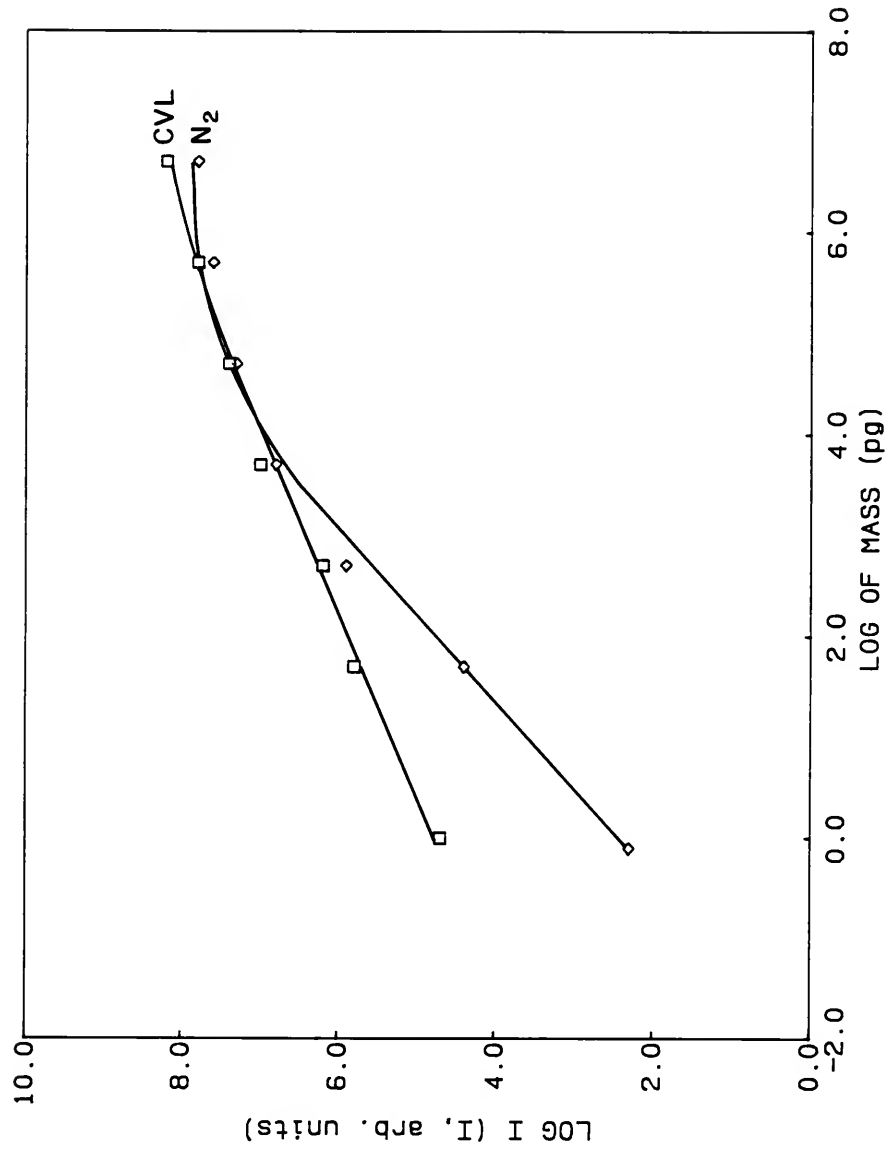
CVL
N_2
LOG I (I, arb. units)
LOG OF MASS (pg)
10.0
8.0
6.0
4.0
2.0
0.0
-2.0
0.0
2.0
4.0
6.0
8.0

calibration curves were due to poor background correction caused by a large amount of scatter when using resonance fluorescence.

The Na results were very similar for each laser except for the slopes of the calibration curves. There was a great deal of contamination in the deionized water and reagents used to prepare the standards. This contamination helped to contribute to poor LODs and also to the inconsistent slopes obtained.

These results suggested that the CVL should be further investigated as a pump laser. The furnace needed to be positioned so that it was more accessible to both lasers. The CVL results should improve dramatically if the fiber optic was not required. Even with the lower energy/pulse of the CVL, improved signals would probably result because of the high repetition rate.

CHAPTER 6
CONCLUSIONS

Summary

This work has shown that laser-excited atomic fluorescence with a graphite furnace can provide low detection limits along with a very good analytically useful range. In many cases the detection limits were improved over detection limits for atomic absorption with a graphite furnace. The plain graphite cup with a pyrolytic coating gave the best results for the volatile elements. The graphite tube provided the best results for nonvolatile elements. The enclosed design of the tube furnace was necessary to atomize the refractory elements. The elements that worked the best had a large separation between the excitation and fluorescence wavelengths, because of reduced scatter. The usefulness of this method was shown by the measurement of NBS standards by using aqueous standards for calibration.

The H_2-Ar atmosphere and the Ar atmosphere surrounding the graphite both worked very well. The H_2-Ar atmosphere provided reducing conditions and the Ar atmosphere provide an inert environment for the atomization process. The LP atmosphere did not work very well due to the high diffusion rates of atoms at low pressure.

The copper vapor laser was found to give mixed results. The main problem was the necessity of using a fiber optic to send the laser beam to the furnace. Also, frequency-doubling efficiency was poor when compared to the nitrogen-dye laser system. When using wavelengths in the visible region, the high repetition rate of the CVL provided an equal or improved signal over the nitrogen laser.

Future Work

Some equipment that would be helpful to this system would be a programmable power supply with a temperature feedback system. In this manner, the temperature of the furnace could be more precisely controlled. Also, the graphite furnace could be held constant at the atomizing temperature for an extended period of time (e.g., 7 s). The extended atomization time would insure the complete atomization of refractory elements. A calibrated photodiode could be used to sense the actual graphite temperature. This signal could be sent to the output computer and be used for determining the atomization temperature (37,38). Mechanistic pathways for the atomization could then be determined.

The work with the CVL should be extended by moving the furnace system near the CVL. The full potential of this pump laser has yet to be realized.

For the tube furnace, several things could be tried. First of all, placing the entrance window at the Brewster angle should reduce the scatter considerably. A commercially coated pyrolytic graphite tube should be used. There would be a large reduction in scatter

caused by particles coming off of the graphite; also the atomization process would be more efficient.

A more novel approach is needed for steering the fluorescence into the monochromator. The mirror with a hole drilled in it causes a large loss of fluorescence back through the hole and there is also a large amount of scatter. A better approach might be to aluminize one side of a quartz window while leaving a small area clear. There would still be losses through the clear area but the size of the open area could be precisely controlled. There may also be less scatter than with the drilled hole.

Perhaps the best possibility for the LP atmosphere is in ionization detection (91-93). The furnace could be used to generate atoms which would be excited using stepwise excitation. A strong electric field could then be applied to produce ionization and allow detection. An electron multiplier would be used to measure the electrons or ions. Bekov and Letokhov (93) have found detection limits of one to two orders of magnitude over other spectroscopic techniques. The LP design could be modified for the ionization work.

REFERENCES

1. Winefordner, J.D. J. Chem. Ed. 1978, 55, 72.

2. Sychra, V.; Svoboda, V.; Rubeska, I. "Atomic Fluorescence Spectroscopy," Van Nostrand Reinhold Company Ltd., London, 1975.

3. Winefordner, J.D.; Schulman, S.G.; O'Haver, T.C. "Luminescence Spectrometry in Analytical Chemistry," John Wiley, New York, 1973.

4. Browner, R.F.; Winefordner, J.D. Spectrochim. Acta 1971, 28B, 263.

5. Cooke, D.O.; Dagnall, R.M.; West, T.S. Anal. Chem. 1972, 44, 2255.

6. Davis, L.A.; Krupa, R.J.; Winefordner, J.D. Analyt. Chim. Acta 1985, 173, 51.

7. Ullman, A.H.; Pollard, B.D.; Boutilier, G.D.; Bateh, R.P.; Hanley, P.; Winefordner, J.D. Anal. Chem. 1979, 51, 2382.

8. Webb, J.P. Anal. Chem. 1972, 44, 30A.

9. Allkins, J.R. Anal. Chem. 1975, 47, 752A.

10. Steinfield, J.I. CRC Crit. Rev. Anal. Chem. 1975, 5, 225.

11. Omenetto, N.; Human, H.G.C. Spectrochim. Acta 1984, 39B, 1333.

12. Green, R.B.; Travis, J.C.; Keller, R.A. Anal. Chem. 1976, 48, 1954.

13. Epstein, M.S.; Bayer, S.; Bradshaw, J.; Voightman, E.; Winefordner, J.D. Spectrochim. Acta 1980, 35B, 233.

14. Kachin, S.V.; Smith, B.W.; Winefordner, J.D. Appl. Spectrosc. 1972, 26, 606.

15. Neuman, S.; Kriese, M. Spectrochim. Acta 1974, 29B, 127.

16. Bolshov, M.A.; Zybin, A.V.; Zybina, L.A.; Koloshnikov, V.G.; Majorov, I.A. Spectrochim. Acta 1976, 31B, 493.

17. Hohimer, J.P.; Hargis, Jr., P.J. Appl. Phys. Lett. 1977, 30, 344.

18. Bolshov, M.A.; Zybin, A.V.; Koloshnikov, V.G.; Vasnetsov, M.V. Spectrochim. Acta 1981, 36B, 345.

19. Bolshov, M.A.; Zybin, A.V.; Smirenkina, I.I. Spectrochim. Acta 1981, 36B, 1143.

20. Miziolek, A.W.; Willis, R.J. Opt. Lett. 1981, 6, 528.

21. Wittman, P.K. Ph.D. Dissertation, Univ. of Florida, 1982.

22. Human, H.G.C.; Omenetto, N.; Cavalli, P.; Rossi, G. Spectrochim. Acta 1984, 39B, 345.

23. Tilch, J.; Falk, H.; Paetzold, H.J.; Mon, P.G.; Schmidt, K.P. Colloquium Spectroscopium Internationale XXIV, Garmish Parkenkirchen, FRG, September 15-25, 1985.

24. Archangelsky, B.V.; Gonchakov, A.S.; Grazhulene, S.S. Colloquium Spectroscopium Internationale XXIV, Garmish Parkenkirchen, FRG, September 15-25, 1985.

25. Dittrich, K.; Stark, H.J. Colloquium Spectroscopium Internationale XXIV, Garmish Parkenkirchen, FRG, September 15-25, 1985.

26. Epstein, M.S.; Nikdel, S.; Bradshaw, J.D.; Kosinski, M.A.; Bower, J.N.; Winefordner, J.D. Anal. Chim. Acta 1980, 113, 221.

27. Uchida, H.; Kosinski, M.A.; Winefordner, J.D. Spectrochim. Acta 1983, 38B, 5.

28. Martellucci, S.; Chester, A.N., eds. "Analytical Laser Spectroscopy," Vol. 119, NATO ASI Series, Series B, Physics, Plenum Press, New York, 1985.

29. Fujiwara, K.; Omenetto, N.; Bradshaw, J.D.; Bower, J.N.; Nikdel, S.; Winefordner, J.D. Spectrochim. Acta 1979, 34B, 317.

30. Langmyhr, F.J. Talanta 1977, 24, 277.

31. Mitchell, A.C.G.; Zemansky, M.W. "Resonance Radiation and Excited Atoms," Cambridge University Press, New York, 1971.

32. Campbell, W.C.; Ottaway, J.M. Talanta 1974, 21, 837.

33. Aggett, J.; Sprott, A.J. Anal. Chim. Acta 1974, 72, 49.

34. Fuller, C.W. Analyst (London) 1974, 99, 739.

35. Fuller, C.W. Analyst (London) 1975, 100, 229.

36. Torsi, G.; Tessari, G. Anal. Chem. 1973, 45, 1812.

37. Sturgeon, R.E.; Chakrabarti, C.L.; Langford, C.H. Anal. Chem. 1976, 48, 1792.

38. Sturgeon, R.E.; Chakrabarti, C.L. Prog. Anal. At. Spectrosc. 1978, 1, 5.

39. Sturgeon, R.E.; Chakrabarti, C.L.; Maines, I.S. Anal. Chem. 1975, 47, 1240.

40. Sturgeon, R.E.; Chakrabarti, C.L.; Bertels, P.C. Anal. Chem. 1975, 47, 1250.

41. Runnels, J.H.; Merryfield, R.; Fisher, H.B. Anal. Chem. 1975, 47, 1258.

42. L'vov, B.V.; Bayunov, P.A.; Ryabchuk, G.N. Spectrochim. Acta 1981, 36B, 397.

43. Wendl, W.; Muller-Vogt, G. Spectrochim. Acta 1984, 39B, 237.

44. L'vov, B.V. "Atomic Absorption Spectrochemical Analysis," Adam Hilger Ltd., London, 1970.

45. L'vov, B.V. Pure Appl. Chem. 1970, 23, 11.

46. L'vov, B.V. Spectrochim. Acta 1978, 33B, 153.

47. Holcombe, J.A.; Rayson, G.D. Prog. Anal. At. Spectrosc. 1983, 6, 225.

48. Holcombe, J.A.; Rayson, G.D.; Akerlind, N. Spectrochim. Acta 1982, 37B, 319.

49. Sturgeon, R.E.; Chakrabarti, C.L. Anal. Chem. 1977, 49, 1101.

50. L'vov, B.V. Spectrochim. Acta 1969, 24B, 53.

51. Manning, D.C.; Ediger, R.D. At. Absorpton. Newslett. 1976, 15, 421.

52. Sturgeon, R.E.; Chakrabarti, C.L. Anal. Chem. 1977, 49, 90.

53. Katz, A.; Taitel, N. Talanta 1977, 24, 132.

54. Yasuda, S.; Kakiyama, H. Anal. Chim. Acta 1977, 89, 369.

55. Rayson, G.D.; Holcombe, J.A. Anal. Chim. Acta 1982, 136, 249.

56. Winefordner, J.D.; Vickers, T.J. Anal. Chem. 1964, 36, 161.

57. Browner, R.F. Analyst 1974, 99, 617.

58. Winefordner, J.D. Chem. Tech. 1975, 5, 123.

59. Winefordner, J.D., ed. "Trace Analysis, Spectroscopic Methods for Elements," John Wiley, New York, 1976.

60. Omenetto, N.; Winefordner, J.D. Prog. Anal. At. Spectrosc. 1979, 2, 1.

61. Omenetto, N.; Winefordner, J.D. In Ch. 4 of "Analytical Laser Spectroscopy," Omenetto, N., ed., John Wiley, New York, 1979.

62. L'vov, B.V. J. Engng. Phys. 1959, 2(2), 441.

63. Massmann, H. Spectrochim. Acta 1968, 23B, 215.

64. West, T.S.; Williams, T.K. Anal. Chim. Acta 1969, 45, 27.

65. Amos, M.D.; Bennet, D.A.; Brodie, K.G.; Lung, P.W.Y.; Matousek, J.P. Anal. Chem. 1971, 43, 211.

66. Molnar, C.J.; Reeves, R.D.; Winefordner, J.D.; Glenn, M.J.; Ahlstrom, J.R.; Savory, J. Appl. Spectrosc. 1972, 26, 606.

67. Winefordner, J.D. Pure Appl. Chem. 1971, 23, 35.

68. Kirkbright, G.F. Analyst 1971, 96, 609.

69. Winefordner, J.D.; Vickers, T.J. Anal. Chem. 1972, 44, 150R.

70. Greenlees, G.W.; Clark, D.L.; Kaufman, S.L.; Lewis, D.A.; Tonn, J.F.; Broadhurst, J.H. Opt. Commun. 1977, 23, 236.

71. Pan, C.L.; Prodan, J.V.; Fairbank, Jr., W.M.; She, C.Y. Opt. Lett. 1980, 5, 459.

72. SCR 20-250 Power Supply Manual, Electronics Measurements, Neptune, NJ.

73. Smith, B.W.; Parsons, M.L. J. Chem. Ed. 1973, 50, 679.

74. Zatka, V.J. Anal. Chem. 1978, 50, 538.

75. Manning, D.C.; Slavin, W. Anal. Chem. 1978, 50, 1234.

76. Renshaw, G.D. At. Absorption Newslett. 1973, 12, 158.

77. L'vov, B.V.; Pelieva, L.A. Can. J. Spectrosc. 1978, 23, 1.

78. Gregoire, D.C.; Chakrabarti, C.L. Spectrochim. Acta 1982, 37B, 11.

79. Thompson, K.C.; Godden, R.G.; Thomerson, D.R. Anal. Chim. Acta 1975, 74, 289.

80. "The Guide to Techniques and Applications of Atomic Spectroscopy," Perkin-Elmer Technical Publication, Norwalk, CT, 1983.

81. Suzuki, M.; Ohta, K.; Yamakita, T.; Katsuno, T. Spectrochim. Acta 1981, 36B, 679.

82. Sacchi, C.A.; Svelto, O. In Ch. 1 of "Analytical Laser Spectroscopy," Omenetto, N., ed., John Wiley, New York, 1979.

83. Walter, W.T.; Solimene, N.; Piltch, M.; Gould, G. IEEE J. Quant. Elect. 1966, QE-2, 474.

84. Model 251 Copper Vapor Laser Manual, Plasma Kinetics Inc., Pleasanton, CA, 1986.

85. Grove, R.E. Laser Focus Magazine 1982, 18, 45.

86. Hargrove, R.S.; Kan, T. IEEE J. Quant. Elect. 1977, QE-13, 28.

87. Data Sheet from Plasma Kinetics, Pleasanton, CA.

88. Hargrove, R.S.; Kan, T. IEEE J. Quant. Elect. 1980, QE-16, 1108.

89. SR 265 Control Program Manual, Stanford Research Systems Inc., Palo Alto, CA, 1985.

90. Laser Dyes Manual, Exciton, Dayton, OH, 1986.

91. Letokhov, V.S. "Chemical and Biochemical Applications of Lasers," Vol. 5, Moore, C.B., ed., Academic Press, New York, 1980.

92. Hurst, G.S.; Payne, M.G.; Kramer, S.D.; Young, J.P. Rev. Mod. Phys. 1979, 51, 767.

93. Bekov, G.I.; Letokhov, V.S. Appl. Phys. 1983, B30, 161.

BIOGRAPHICAL SKETCH

Douglas Edmon Goforth was born March 22, 1960, in Alamogordo, New Mexico. In 1972 his family and he moved to Dana, Indiana, where he graduated from South Vermillion High School in 1978. In 1982 he obtained a Bachelor of Science degree from the New Mexico Institute of Mining and Technology in Socorro, New Mexico. In August of 1982 he entered the Graduate School at the University of Florida in Gainesville, Florida.

I certify that I have read this study and that in my opinion it conforms to acceptable standards of scholarly presentation and is fully adequate, in scope and quality, as a dissertation for the degree of Doctor of Philosophy.

James D. Winefordner, Chairman
Graduate Research Professor of Chemistry

I certify that I have read this study and that in my opinion it conforms to acceptable standards of scholarly presentation and is fully adequate, in scope and quality, as a dissertation for the degree of Doctor of Philosophy.

John G. Dorsey
Associate Professor of Chemistry

I certify that I have read this study and that in my opinion it conforms to acceptable standards of scholarly presentation and is fully adequate, in scope and quality, as a dissertation for the degree of Doctor of Philosophy.

Eric R. Allen
Professor of Environmental Engineering

This dissertation was submitted to the Graduate Faculty of the Department of Chemistry in the College of Liberal Arts and Sciences and to the Graduate School and was accepted as partial fulfillment of the requirements for the degree of Doctor of Philosophy.

August, 1986

Dean, Graduate School